ISTANBUL TECHNICAL UNIVERSITY ★ GRADUATE SCHOOL

PARAMETRIC INVESTIGATION OF MECHANICAL PROPERTIES OF AUXHEX UNIT CELL SANDWICH STRUCTURES

M.Sc. THESIS

Kadircan SAYGI

Department of Aeronautics and Astronautics Engineering

Aeronautics and Astronautics Engineering Programme

JULY 2024

ISTANBUL TECHNICAL UNIVERSITY ★ GRADUATE SCHOOL

PARAMETRIC INVESTIGATION OF MECHANICAL PROPERTIES OF AUXHEX UNIT CELL SANDWICH STRUCTURES

M.Sc. THESIS

Kadircan SAYGI
(511201169)

Department of Aeronautics and Astronautics Engineering

Aeronautics and Astronautics Engineering Programme

Thesis Advisor: Asst. Prof. Kaan YILDIZ

JULY 2024

İSTANBUL TEKNİK ÜNİVERSİTESİ ★ LİSANSÜSTÜ EĞİTİM ENSTİTÜSÜ

AUXHEX BİRİM HÜCRELİ SANDVİÇ YAPILARIN MEKANİK ÖZELLİKLERİNİN PARAMETRİK OLARAK İNCELENMESİ

YÜKSEK LİSANS TEZİ

Kadircan SAYGI
(511201169)

Uçak ve Uzay Mühendisliği Anabilim Dalı

Uçak ve Uzay Mühendisliği Programı

Tez Danışmanı: Dr. Öğr. Üyesi Kaan YILDIZ

TEMMUZ 2024

Kadircan SAYGI, a M.Sc. student of ITU Graduate School student ID 511201169 successfully defended the thesis entitled “PARAMETRIC INVESTIGATION OF MECHANICAL PROPERTIES OF AUXHEX UNIT CELL SANDWICH STRUCTURES”, which he prepared after fulfilling the requirements specified in the associated legislations, before the jury whose signatures are below.

Thesis Advisor :	**Asst. Prof. Kaan YILDIZ** Istanbul Technical University	....
Jury Members :	**Assoc. Prof. Seher EKEN** Istanbul Technical University	....
	Asst. Prof. Fatih USTA Gebze Technical University	....

Date of Submission : **24 May 2024**
Date of Defense : **01 July 2024**

To my family,

FOREWORD

First of all, I am deeply grateful to my thesis advisor Asst. Prof. Dr. Kaan Yildiz for his invaluable guidance and continuous support throughout this thesis. His experience and expertise have been a constant source of support.

Dr. Kadir Gunaydin is the other person I would like to offer my sincerest gratitude to. His invaluable mentorship for finite element method have been beneficial in the development of this thesis.

I wouldn't be here without the constant love and understanding of my family. They are my greatest source of strength. Special thanks to my family for their unwavering love!

Lastly, my deepest thanks go to Hilal Erkoc whose endless support and precious advices have been foundation for everything I achieve.

July 2024

Kadircan SAYGI
Astronautical Engineer

TABLE OF CONTENTS

ABBREVIATIONS

2D	: Two Dimensional
3D	: Three Dimensional
AuxHex	: Auxetic Hexagonal
CFR	: Carbon Fiber Reinforced
D	: Depth
EA	: Energy Absorption
$EA_{0.1}$	: Energy Absorption at 10% Strain
$EA_{0.25}$	: Energy Absorption at 25% Strain
Eqs.	: Equations
FE	: Finite Element
FEM	: Finite Element Method
GFR	: Glass Fiber Reinforced
H	: Height
W	: Width
YS	: Yield Strength

SYMBOLS

$\mathbf{E}$	: Young's Modulus
ε	: Strain
σ	: Stress
$\mathbf{h_1}$	: Conventional hexagonal cell's length of the non-inclined walls
$\mathbf{l_1}$	: Conventional hexagonal cell's length of the inclined walls
θ_1	: Conventional hexagonal cell's angle
$\mathbf{t_1}$	: Conventional hexagonal cell's wall thickness
$\mathbf{h_2}$	: Re-entrant hexagonal cell's length of the non-inclined walls
$\mathbf{l_2}$	: Re-entrant hexagonal cell's length of the inclined walls
θ_2	: Re-entrant hexagonal cell's angle
$\mathbf{t_2}$	: Re-entrant hexagonal cell's wall thickness
$\mathbf{h_3}$	: Length between conventional and re-entrant hexagonal cells
$\mathbf{t_3}$	: Wall thickness of the length between conventional and re-entrant hexagonal cells
$\mathbf{M_x^i}$	: Bending moment acting on beam for conventional hexagonal cell
$\mathbf{P^i}$	: Force in the x-direction acting on beam
σ_1	: Stress in the x-direction
$\mathbf{b}$	: Depth of the AuxHex unit cell through out-of-plane direction
$\mathbf{E_s}$	: Young's modulus of the parent material
δ_x^i	: Deflection of beam for conventional hexagonal cell
$\mathbf{I^i}$	: Moment of inertia of beam for conventional hexagonal cell
ε_x^i	: Strain of conventional hexagonal cell in x-direction
$\mathbf{M_x^{ii}}$	: Bending moment acting on beam for re-entrant hexagonal cell
$\mathbf{P^{ii}}$	: Force in the x-direction acting on beam for re-entrant hexagonal cell
δ_x^{ii}	: Deflection of beam for re-entrant hexagonal cell
$\mathbf{I^{ii}}$	: Moment of inertia of beam for re-entrant hexagonal cell
ε_x^{ii}	: Strain of re-entrant hexagonal cell in x-direction
ε_x	: Strain of AuxHex cell in x-direction
$\mathbf{E_1}$	: Young's modulus through x-direction for AuxHex cell
$\mathbf{M_{1p}^i}$	: Fully plastic moment of the bending wall
σ_y	: Yield stress of the parent material
$(\sigma_y)_{pl}^i$	: Conventional hexagonal cell's plastic collapse stress
$(\sigma_y)_{pl}^{ii}$	: Re-entrant hexagonal cell's plastic collapse stress

LIST OF TABLES

LIST OF FIGURES

PARAMETRIC INVESTIGATION OF MECHANICAL PROPERTIES OF AUXHEX UNIT CELL SANDWICH STRUCTURES

SUMMARY

In this study, the mechanical properties of the AuxHex structure, which consists of hybrid unit cells obtained by combining the classical hexagonal honeycomb unit cell structure with the auxetic unit cell structure, are investigated under axial compressive loads by changing the geometric parameters. In the studies carried out, it has been observed that the AuxHex structure, which is obtained by hybridizing two different cell structures, has a better strength value against in-plane compressive loads. Before investigating the effect of geometric parameters on the mechanical properties of the AuxHex structure, a validation study was performed by analyzing the AuxHex structure using the ABAQUS 2020 commercial finite element program with an appropriate study in the literature and based on the results of this validation study, the boundary and loading conditions, material properties to be defined, and other variables for finite element models and analyses of other AuxHex structures have been determined. Subsequently, the mechanical properties, including Young's modulus, yield strength, energy absorption capacity under different strain values, and toughness were investigated for nine (9) different geometries of AuxHex sandwich structures by varying geometric parameters such as inclined and non-inclined wall cell lengths, angles, and wall thicknesses that characterize the AuxHex unit cell structure. To analyze the Young's modulus and yield strength among these mechanical properties, both theoretical formulas used in the literature and finite element analysis results were utilized. The results obtained from the finite element analyses were employed to determine and compare the absorbed energy under certain strains and toughness values of nine (9) different AuxHex structures. The force-displacement graphs obtained from the finite element analyses were converted into stress-strain graphs. The resulting stress-strain graphs were integrated by using a curve fitting function in the MATLAB program to obtain the absorbed energies and toughness values at different strains values. These graphs were also useful for determining the Young's modulus and strengths. As a result of all these studies, it was observed that the elastic modulus, yield strength, energy absorption capacity, and toughness of the sandwich structure decreased with increasing inclined and non-inclined wall lengths of AuxHex unit cells. However, it was concluded that all these mechanical properties increased significantly and had a positive effect on the structure with increasing AuxHex unit cell wall thicknesses. Finally, it was concluded that the elastic modulus, yield strength, energy absorption capacity, and toughness of the AuxHex sandwich structure decreased with increasing angle values used to design the AuxHex unit cells, and lastly, the combination of all AuxHex structures' stress-strain graphs in one shows that the collapse behaviour of structure appears to be largely related to the change in the length of non-inclined wall.

AUXHEX BİRİM HÜCRELİ SANDVİÇ YAPILARIN MEKANİK ÖZELLİKLERİNİN PARAMETRİK OLARAK İNCELENMESİ

ÖZET

Geçmişten günümüze, mühendisler ve bilim insanları, istenilen performansı sağlayacak malzemeler ve yapılar geliştirmek için durmaksızın çaba göstermişlerdir. Daha yüksek mukavemet, darbe sönümleme yeteneği, ve hafiflik gibi üstün özelliklere sahip yepyeni malzemeler geliştirilmiştir. Bu sayede, daha önce imkansız olduğu düşünülen ürünler ve yapılar mümkün hale gelmiştir. Sandviç panellerde dolgu görevi gören hücresel petekli yapılar, sağladıkları yüksek mekanik özelliklerle bu çabaların sonucunda elde edilen yapılara bir örnek oluşturur.

Teknolojinin ilerlemesiyle mühendislik, birçok alanda çığır açmaktadır. Gelişen teknolojiyle beraber bilgisayar destekli mühendislik çalışmaları artmış, artan bu çalışmalarla beraber yeni üretim yöntemleri ortaya konmuş ve bu sayede farklı tipte malzemeler ve yapılar ortaya çıkmıştır. Mühendislik anlamında bütün bu gelişmelerin ışığında ortaya çıkan teknolojiler ve yenilikler, farklı teknik alanlarda büyük ölçüde ilerlemeler kaydedilmesine neden olmuştur.

Bu çalışmada, klasik altıgen balpeteği birim hücre yapısının ökzetik birim hücre yapısı ile bir araya getirilmesi sonucu ortaya çıkan hibrit birim hücrelerden oluşan AuxHex yapısının, geometrik parametreleri değiştirilerek eksenel basma yükü altında sergilediği mekanik özellikleri incelenecektir. Hücresel petekli yapılar çoğunlukla sandviç panellerde dolgu malzemesi olarak kullanılmaktadır. Mühendislik uygulamaları için tasarlanan bu düşük yoğunluklu ve hafif yapıların temel amacı, yüksek rijitlik-ağırlık oranı elde etmektir. Düşük yoğunluklu hafif yapılar, özellikle sandviç paneller ve dolgu malzemeleri, havacılık, otomotiv, denizcilik gibi endüstrilerde ve askeri mühendislik uygulamalarında darbe ve patlamaya karşı ezilme dirençleri açısından kritik önem taşır. Sandviç panellerin üst ve alt yüzeyleri, genellikle fiber takviyeli kompozitler veya alüminyum alaşımlar gibi hafif malzemelerden yapılır. Mükemmel mekanik performansı, yüksek mukavemeti ve enerji absorbe etme yeteneği nedeniyle sandviç panellerde kullanılan hücresel yapılar, havacılık ve uzay endüstrilerinde sıklıkla tercih edilir. Hücresel petekli yapıları oluşturan birim hücrelerin tasarım ve optimizasyonu, hücresel yapıların mekanik özelliklerinin geliştirilmesine olanak sağladığından giderek daha popüler bir araştırma konusu haline gelmektedir.

Farklı birim hücre şekillerinin yük altında nasıl deforme olduklarına ve tepki gösterdiklerine bakılarak, bu hücresel yapılar üç kategoriye ayrılabilir: pozitif Poisson oranına sahip olanlar, sıfır Poisson oranına sahip olanlar ve negatif Poisson oranına sahip olanlar. Arılar tarafından ortaya çıkarılan doğal balpetekleri gibi, klasik altıgen şeklindeki balpeteğinden birim hücrelere sahip yapılar pozitif Poisson oranına

sahip malzemelerin başlıca örneklerindendir. Lakin, bu geleneksel altıgen balpeteği yapılarını iyileştirmenin sınırlı olduğu zamanla görülmüştür. Bunun nedeni, optimal mekanik özellikler için tasarımları fazlaca esnetebilme imkanı olmamasıdır. Ökzetik malzemeler ise pozitif Poisson oranına sahip klasik malzemelere kıyasla sıra dışı bir mekanik davranış sergiledikleri için bu sorunun üstesinden gelmede önemli bir rol oynarlar. Bu tip malzemeler, çekme yükleri altında yanal genişleme ve basma yükleri altında yanal daralma özelliği gösterdiklerinden negatif Poisson oranına sahip malzemeler olarak da bilinir. Bu özellik, çekirdek ve dolgu malzemesi olarak kullanıldıklarında birçok avantaja sahip olmalarını sağlar. Negatif Poisson oranına sahip ilk sentetik malzeme 1987 yılında Lake tarafından tanıtılmıştır. Bu malzemeleri tanımlamak içinse 1991 yılında Evans tarafından "ökzetik" kelimesi ortaya atıldı. Negatif Poisson oranına sahip ökzetik yapılar, geleneksel pozitif Poisson oranına sahip olanların ötesinde benzersiz özelliklere sahip oldukları için metamalzemeler olarak da adlandırılır. Literatürdeki pozitif veya negatif Poisson oranına sahip yapılarla ilgili çalışmalara rağmen, zaman içerisinde hem pozitif Poisson oranı hem de negatif Poisson oranı özelliklerini gösteren hücresel yapılara ihtiyaç duyulmuştur.

Bahsi geçen klasik altıgen şeklindeki birim hücrelerle ökzetik altıgen birim hücrelerle hibritleyerek ortaya çıkan AuxHex hücre yapısı hem pozitif Poisson oranına sahip hem de negatif Poisson oranına sahip yapıların farklı avantajlarından yararlanmak için tasarlanmıştır. Yapılan çalışmalarda iki farklı hücre yapısının bir araya getirilmesiyle ortaya çıkan AuxHex yapısının düzlem içi basma yüklerine karşı daha iyi bir dayanım değeri verdiği gözlemlenmiştir. Bu bağlamda AuxHex hücrelerinden oluşan yapıların tasarım parametrelerinin farklı değerler alarak bu değişikliklerin yapının mekanik özelliklerine etkisi gözlemlenmiştir. Bilindiği kadarıyla AuxHex birim hücresinin farklı değerlerdeki tasarım parametrelerinin ve bunların mekanik özelliklere etkisi detaylı olarak incelenmemiştir. AuxHex yapısının hem klasik altıgen şeklindeki balpeteği hücrelerin hem de ökzetik altıgen hücrelerin avantajlarından yararlanmak üzere tasarlanmış olması nedeniyle bu çalışma, tasarım parametrelerinin etkilerini ve birim hücrenin mekanik özelliklerinin nasıl iyileştirilebileceğini incelemeyi amaçlamaktadır. Sonuçlar, birim hücreyi tanımlayan tasarım parametrelerinin değiştirilmesiyle mekanik özelliklerin ne kadar geliştirilebileceğini göstermektedir. Bu sayede AuxHex yapılar için optimum tasarım çözümleri geliştirilebilmesi amaçlanmaktadır.

Çeşitli tasarım parametrelerin AuxHex yapısının mekanik özelliklerine etkisini incelemeden önce literatürdeki uygun bir çalışma ile AuxHex yapısı, ticari sonlu elemanlar analiz programı ABAQUS 2020 yardımı ile simüle edilerek bir doğrulama çalışması gerçekleştirilmiştir ve bu doğrulama çalışmasıyla elde edilecek sonuçlar sayesinde diğer AuxHex yapılarının sonlu elemanlar modelleri ve analizleri için sınır ve yükleme koşulları, tanımlanacak malzeme özellikleri vb. değişkenler belirlenmiştir. Ardından AuxHex birim hücre yapısını ortaya çıkaran eğik duvar hücre uzunlukları, düz duvar hücre uzunlukları, açıları ve duvar kalınlıkları gibi geometrik parametreleri değiştirilerek dokuz (9) farklı geometrideki AuxHex sandviç yapılarındaki elastisite modulü, basma yükü altındaki dayanımı, farklı birim şekil değiştirme değerlerindeki enerji emme kapasitesi ve tokluğu gibi mekanik özellikleri incelenmiştir. Bu mekanik özelliklerden elastisite modulünü ve basma yükü altındaki dayanımını analiz edebilmek için hem literatürde kullanılan teorik formüllerden hem de sonlu elemanlar analiz sonuçlarından faydalanılmıştır. Dokuz (9) farklı geometrideki AuxHex yapısının farklı birim şekil değiştirme değerlerindeki absorbe edilen enerji ve tokluk değerini bulmak ve kıyas yapabilmek içinse sonlu elemanlar programından elde edilen sonuçlar kullanılmıştır. Sonlu elemanlar analizleri sonucu elde edilen kuvvet-yer değiştirme grafikleri gerilme-birim şekil değiştirme grafiklerine dönüştürülmüştür. Ortaya çıkan farklı gerilme-birim şekil değiştirme grafikleri MATLAB programında eğri uydurma fonksiyonuyla beraber integre edilerek farklı birim şekil değiştirme değerlerindeki absorbe edilen enerjiler ve tokluk değerleri elde edilmiştir. Bu grafikler aynı zamanda dokuz farklı AuxHex modelinin elastisite modullerini ve basma kuvveti altındaki dayanımlarını bulmak için de faydalı olmuştur.

Yapılan bütün bu çalışmalar neticesinde artan düz ve eğik duvar uzunluklarıyla beraber sandviç yapısının elastiste modulünün, basma kuvvetleri altındaki dayanımının, enerji absorbe edebilme yeteneğinin ve tokluğunun düştüğü gözlemlenmiştir. Lakin, artan birim hücre duvar kalınlıklarıyla beraber bütün bu mekanik özelliklerin ciddi derece artış gösterdiği ve yapıya pozitif etki ettiği sonucuna varılmıştır. Ek olarak birim hücreleri tasarlayabilmek için kullanılan açı değerinin artmasıyla AuxHex sandviç yapısının elastiste modulünün, basma kuvvetleri altındaki dayanımının, enerji absorbe edebilme yeteneğinin ve tokluğunun düştüğü sonucuna varılmıştır. Son olarak, dokuz farklı AuxHex sandviç yapısının gerilme-birim şekil değiştirme grafiklerinin bir arada gösterilmesiyle, yapıdaki çökme davranışının büyük ölçüde düz duvarların uzunluğundaki değişime bağlı olduğu görülmektedir.

1. INTRODUCTION

Lattice structures also known as cellular solids are widely used as core material in sandwich panels. The primary goal of low-density lightweight structures designed for engineering applications is to achieve high stiffness-to-weight ratios. Upper and lower face-sheets of sandwich structures are typically made of lightweight materials such as fiber-reinforced composites or aluminum alloys. The core structure, commonly used in sandwich panels, is widely favored in the aerospace and space industries due to its excellent mechanical performance, including high strength and energy absorption capability. Design and optimization of unit cells which create core becomes more popular research subject because it allows to have tunable mechanical properties of core structures.

1.1 Literature Review

Nowadays, design and optimization of an unit cell of sandwich core structure is a hot topic with a lot of new developments happening. This topic catchs researchers' attention since its usage become popular in engineering divisions such as aerospace, automotive, marine, and military applications and one of the examples for aerospace applications is shown in Figure 1.1.

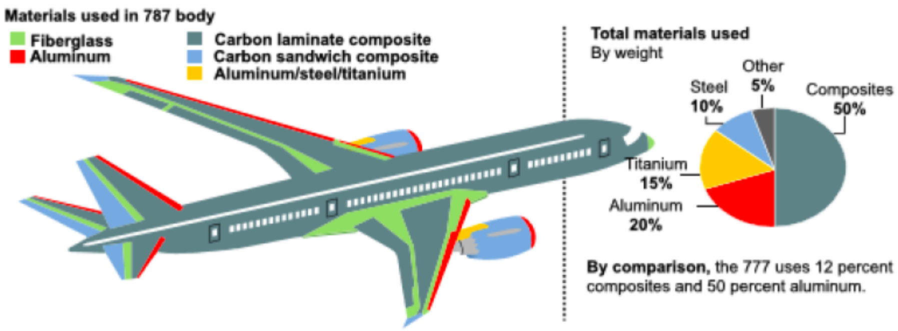

Figure 1.1 : Sandwich structure of Boeing 787 aircraft [1].

Researchers have investigated many designs for unit cells using different shapes. Unit cell design is crucial since it is constituent part of sandwich structure (see Figure 1.2). By looking at how the different unit cell shapes deform and react under loads, these lattice structures can be classified into three categories: those with positive Poisson's ratio (PPR), those with zero Poisson's ratio (ZPR), and those with negative Poisson's ratio (NPR) [14]. These three different classifications are visually explained in Figure 1.3.

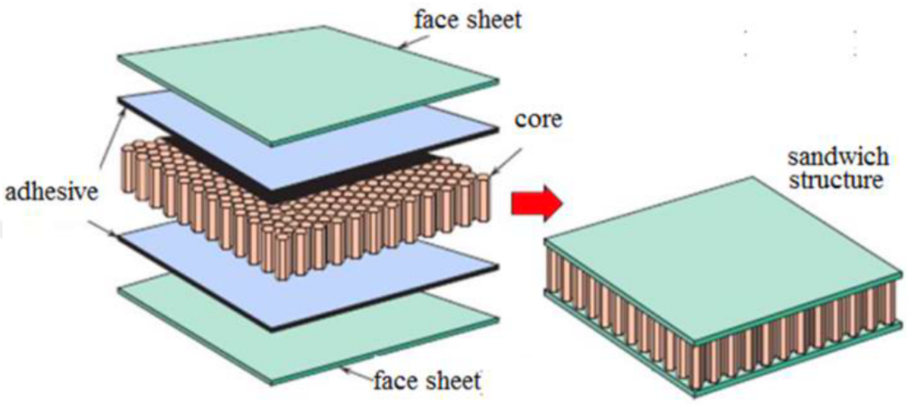

Figure 1.2 : Constituent parts of sandwich structure [2].

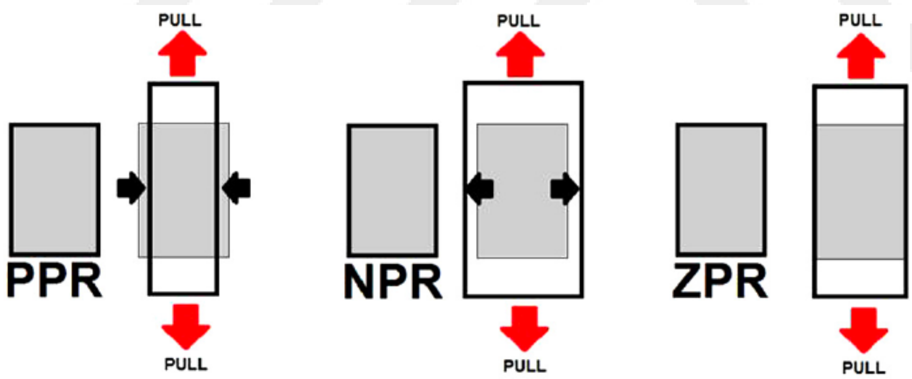

Figure 1.3 : Deformation response of PPR, NPR and ZPR in 2D [3].

Just like natural honeycombs built by bees, hexagonal structures are a prime example of materials with PPR. These materials are popular in research because they're very stiff and strong when pushed in from the side. Researchers have done many studies, both in theory and with experiments, to understand the mechanical properties and failure mechanisms of hexagonal honeycomb cores and sandwich panels made from different raw materials under stress. Zhang et al. have searched for conventional hexagonal honeycomb core's collapse mechanism under load in compression and shear [15].

The study has shown collapse behaviour with various engineering phenomenas such as buckling, de-bonding and fracture of hexagonal honeycomb's cell walls. Ashby et al. have stated that hexagonal honeycomb core is an great energy absorbing material since under large amount of strain without increased stress levels, this core absorbs considerable amount of energy [16]. In-plane and out-of-plane energy absorption capability of polymeric honeycomb hexagonal sandwich structure under low-velocity impact was investigated with various cores with a modified higher-order shear deformation theory and by using FEM application and, it was found the influence of geometrical design parameters [17]. The influence of structural parameters on collapse and crashworthiness characteristics of isotropic hexagonal honeycomb core sandwich panels was investigated by three-point bending and in-panel compression tests by Sun et al. [18] and this study helps to understand how to make even better hexagonal honeycomb sandwich structures that can withstand crashes. Khan et al. introduced a method that combines quasi-static compression tests with digital image analysis to measure deformation fields and analyze the deformation mechanisms of aluminum honeycombs at both the global and local levels [19]. Wang et al. [20] have designed a new hexagonal honeycomb structure with perforations in it and studied how the crushing strength of this structure changes as the number of perforations is changed. This investigation used both physical experiments and computer simulations (by FEM) for analysis. Nevertheless, it's shown that there's a limitation on how better conventional hexagonal honeycomb structures because there's not much room to adjust the design for optimal mechanical properties [21]. Fu et al. [22] created improved auxetic cells by incorporating diamond-shaped units (rhombus) into regular auxetic cells in various orientations. Their design showed significant improvement in both the modulus of elasticity and critical buckling strength.

While great number of studies have explored lattice structures with NPR (see Figure 1.4), the first man-made foam exhibiting this property was introduced by Lake in 1987 [23].

Recent researches have focused on re-entrant hexagonal structures, which exhibit a higher NPR. These structures are also known as auxetic materials [24]. Subsequently, Evans coined the terminology "auxetic" in 1991 to describe these materials [25].

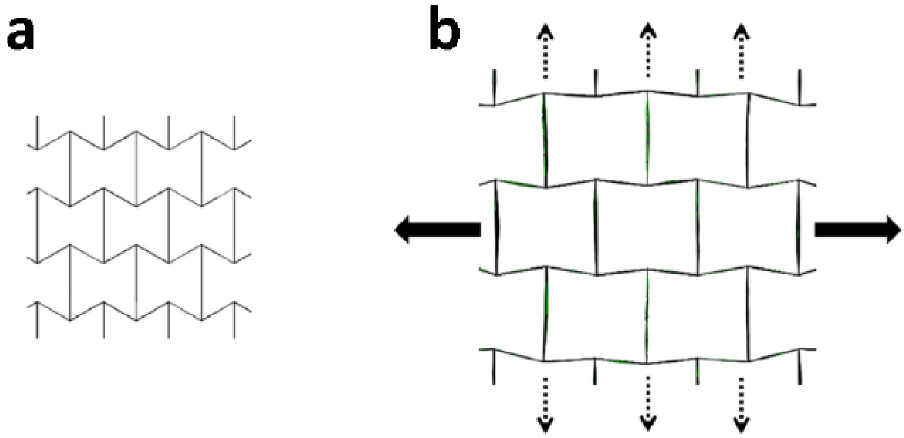

Figure 1.4 : (a) Undeformed and b) deformed behaviour of re-entrant auxetic structure [4].

Auxetic structures offer clear benefits in absorbing energy and isolating vibrations unlike conventional cellular solids [26,27]. For example, the study by Zhang et al. [28] has been conducted for a detailed analysis of how auxetic materials behave when stretched to large deformations. Additionally, a theoretical model has been created based on the simplified picture of how these materials deform. This model takes into account the non-linear way the cell walls deform permanently. Huang et al. [24] studied the in-plane mechanical properties of NPR honeycombs. Their design incorporates an auxetic hexagonal unit cell and a thin plate and to analyze this structure, they employed both theoretical analysis and FE simulations. Pros of different materials were also discussed in the literature. For instance, Gunaydin et al. [29] have discussed the effect of using multiple materials within hexagonal and re entrant (auxetic) cellular structures. With the usage of three different material types including nylon, CFR nylon and GFR nylon, the study has proved that using a combination of materials (multi-material approach) significantly improved the performance of the re-entrant cellular structures. Compared to structures made entirely of nylon, the multi-material design increased the specific energy absorption by 60 percent, compressive strength by 104 percent, and modulus value by 201 percent. Meanwhile, some researchers focused on enhancing the mechanical properties of auxetic materials while preserving their negative Poisson's ratio behavior [30]. For example, researches have proposed a novel re-entrant auxetic structure, considering how different parts of the structure respond to stress [31]. To analyze this novel design, they developed a more accurate theoretical model based on principles of energy theorems. This model comprehensively accounts for how the structure bends, deforms by shearing effects, and membrane effects. The focus of Chen et al. [32]'s research was to determine the in-plane elasticity equations for anti-tetrachiral lattices. They achieved this by calculating the equations and validating them through comparisons with experimental results. Fu et al. [22] created improved auxetic cells by incorporating diamond-shaped units (rhombus) into regular auxetic cells in various orientations. Their design showed significant improvement in both the modulus of elasticity and critical buckling strength.

Despite all these efforts, there has been a need for cellular structures that exhibit both PPR and NPR properties over time. In this context, one of the first studies was carried out by Brocolo et al. [3]. They have focused on that the AuxHex hybrid metastructure is achieved by combining conventional and auxetic hexagonal unit cells as shown in Figure 1.5. This design allows for variable Poisson's ratios (positive, zero, and negative) to be obtained by adjusting its geometric parameters and for enhanced in-plane compressive strength. Xu et al. [12] derived theoretical formulas for the modulus of elasticity and collapse stress of the AuxHex structure. They then validated these theoretical calculations by comparing them with the results of experiments performed on nylon samples and the results of FEM applications. Parsons et al. [33] created AuxHex structures by using aluminum and titanium materials, achieving tunable positive or negative thermal expansion coefficients in two perpendicular directions. This opens up new possibilities for applications of hybrid honeycombs. Additionally, they confirmed the thermal expansion properties of these metastructures through experiments.

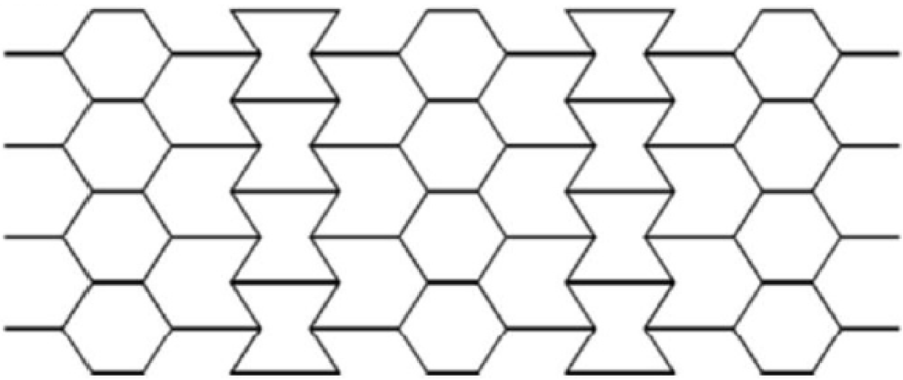

Figure 1.5 : 2D AuxHex structure [3].

1.2 Purpose of Thesis

Herein, parametric investigation of mechanical properties of sandwich structures with AuxHex unit cells is conducted. Due to author's knowledge, the investigation of various geometric parameters of AuxHex unit cell and its effect on mechanical properties were not discussed in detail. Since AuxHex is designed to take advantage of the distinct advantages of both conventional hexagonal honeycomb and auxetic re-entrant cells, this study aims to see the effect of design parameters and how to improve mechanical properties of unit cell of AuxHex. The results show how far the mechanical properties can be tailored and advanced by varying geometric parameters of unit cell design. This facilitates the development of optimal design solutions for AuxHex structures by employing different values for the geometric parameters.

2. LATTICE STRUCTURES

This section delves into a detailed explanation of the classical conventional honeycomb-shaped unit cells and re-entrant auxetic unit cells that give rise to the AuxHex unit cell.

2.1 Conventional Hexagonal Lattices (Honeycombs)

Inspired by the hexagonal structures found in natural honeycombs built by bees, honeycomb cores, also known as cellular or open-cell cores, utilize various geometries. However, the most common and well-studied design employs hexagonal cells, as illustrated in Figure 2.1. The hexagonal arrangement of the honeycomb core offers a combination of desirable properties: low density, exceptional out-of-plane compressive strength, and high resistance to out-of-plane shear forces [6].

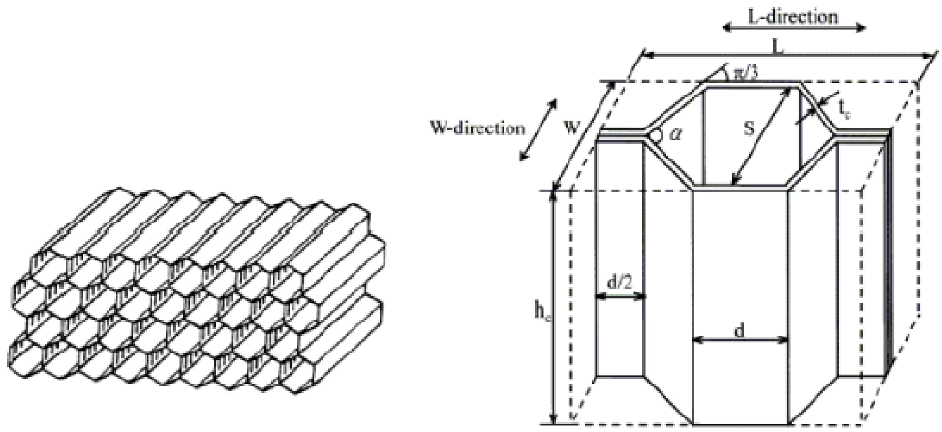

Figure 2.1 : Honeycomb structure and its geometry [5,6].

A key parameter in defining a honeycomb core is the cell size. This is determined by the diameter of the largest circle that can be inscribed within the cell walls, as depicted in Figure 2.2. The figure also illustrates the dimensions (length L, width W, and thickness T) of a typical hexagonal honeycomb cell. However, the achievable cell configurations are ultimately limited by the thickness and stiffness of the sheet material used for fabrication.

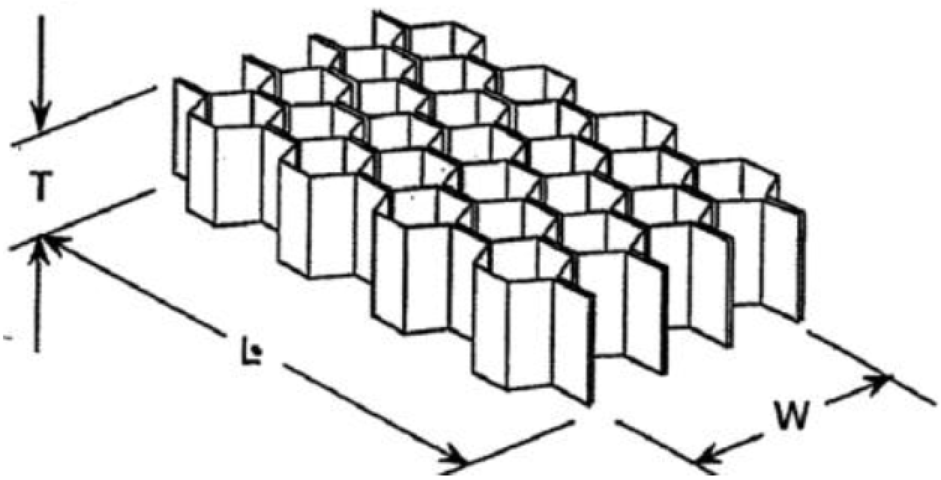

Figure 2.2 : Honeycomb structure's directions [7].

Honeycomb structures in engineering applications experience compressive loading in either the in-plane (X_1 or X_2 directions) or out-of-plane (X_3 direction) as illustrated in Figure 2.3. When loaded in-plane, the cell walls bend due to their lower compressive strength compared to out-of-plane loading. This is because under out-of-plane compression, the cell walls experience axial extension or compression, leading to a higher overall strength.

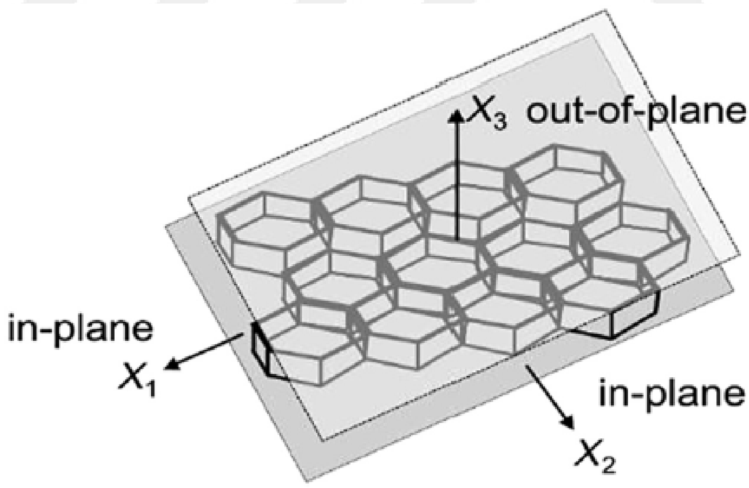

Figure 2.3 : Visualization of the in-plane (X_1 and X_2) and out-of-plane (X_3) loading directions with respect to the honeycomb's geometry [8].

2.2 Re-entrant Auxetic Lattices

Under tensile loading, most materials exhibit a positive Poisson's ratio, meaning they become thinner in the direction perpendicular to the applied force. This is readily observed when stretching an elastic band. This behavior is so prevalent in nature that PPR seems to be the default expectation for material response. Conventional honeycomb structures mentioned in previous sub-chapter are the ones that exhibiting normal expectation of material deformation, PPR. By implementing various design modifications to the hexagonal honeycomb geometry, it is possible to alter its behavior from exhibiting a PPR to a structure with a negative Poisson's ratio. The discrepancy between PPR and NPR behaviors is illustrated in Figure 1.3 and 2.4.

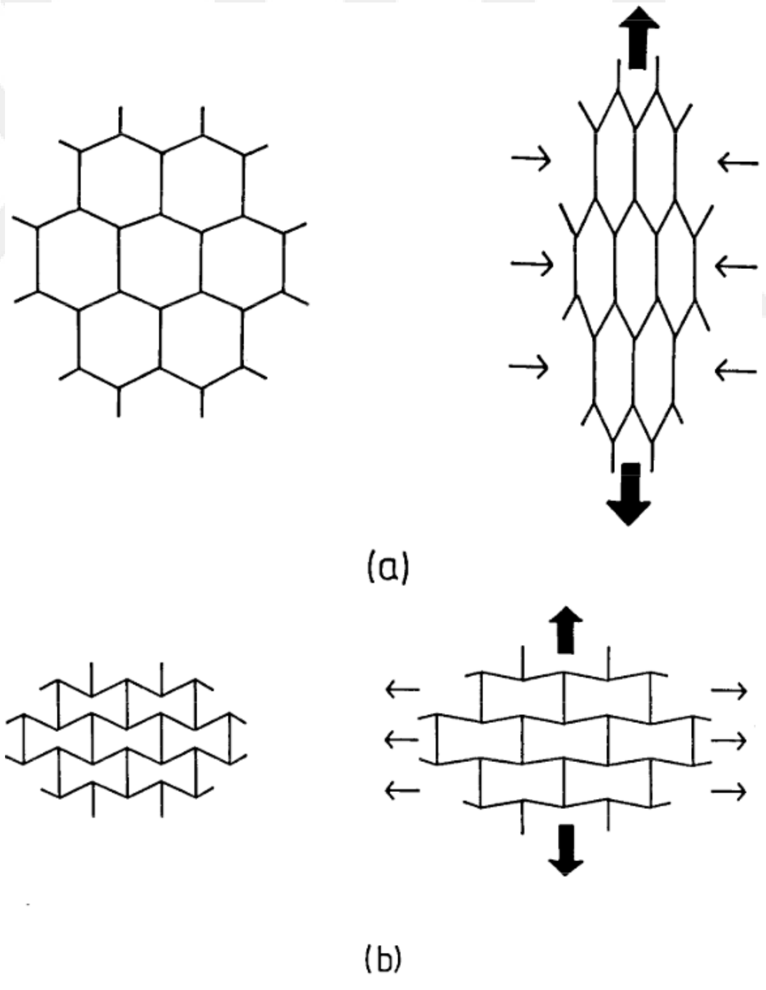

Figure 2.4 : (a) Depicting a schematic of a typical hexagonal honeycomb structure and its deformation under tensile loading, which results in a (PPR) (b) A re-entrant honeycomb exhibiting negative Poisson's ratio behavior [9].

The re-entrant geometry exhibits a NPR, making it the most widely recognized design among auxetic structures. Unlike the conventional hexagonal honeycomb with its characteristic 120° internal angles, the re-entrant structure incorporates a arrow shaped hexagonal honeycomb core. The specific internal angles within this structure can be tailored based on the design requirements.

Figure 2.5 illustrates the distinction between a conventional hexagonal honeycomb structure and a re-entrant auxetic structure. Notably, the Poisson's ratio of the re-entrant geometry is dictated by the specific angles between its cell walls and other geometric parameters [34].

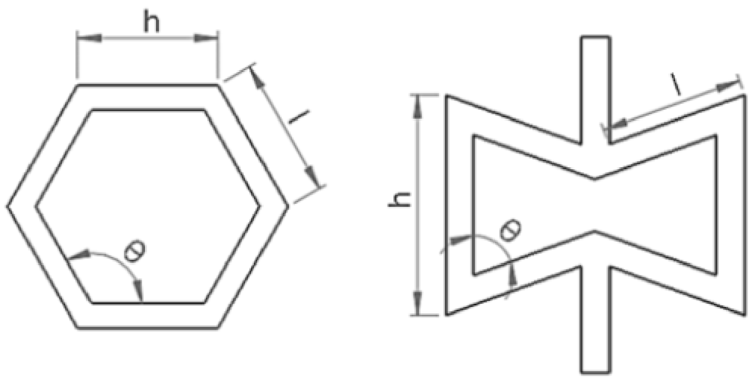

Figure 2.5 : Geometries of classical honeycomb structure's unit cell and re-entrant structure's unit cell [10].

3. AUXHEX UNIT CELL

3.1 Geometrical Description of AuxHex Unit Cell

An AuxHex unit cell is the result of combination of hexagonal unit cell and re-entrant unit cell (auxetic unit cell). The AuxHex lattice structure is shown in Figure 3.1 and Figure 3.2.

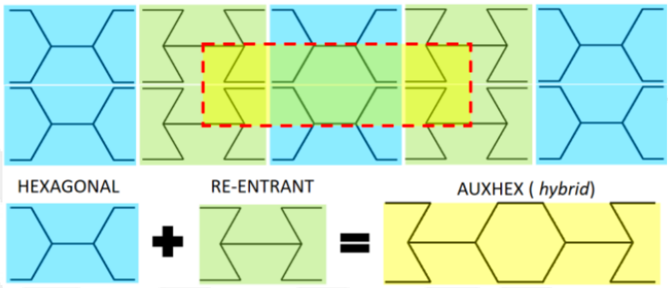

Figure 3.1 : AuxHex unit cell structure, combination of two different type of unit cells [11].

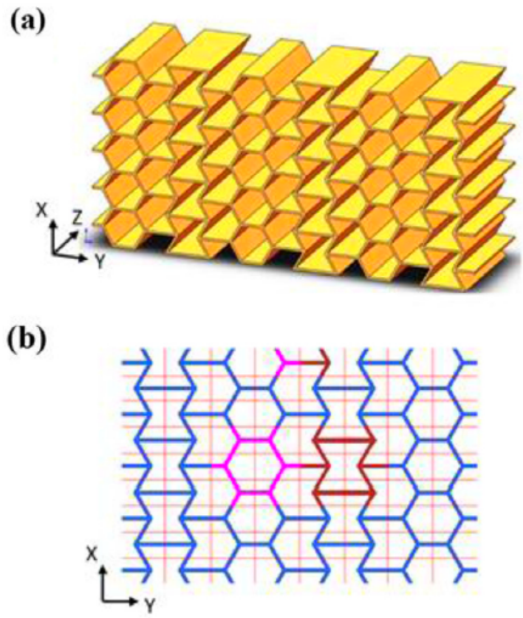

Figure 3.2 : AuxHex unit cell structure: (a) 3D AuxHex structure; (b) 2D AuxHex structure [12].

Unlike the original cells, the combined cell (hybrid cell or AuxHex) allows for more flexibility in design parameters. To understand the exact shape of AuxHex unit cell, some key design parameters are defined and shown in Figure 3.3.

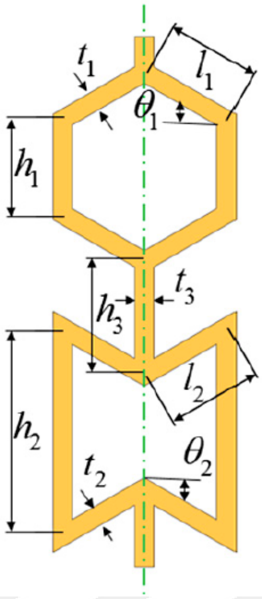

Figure 3.3 : Design parameters information of AuxHex lattice structure [13].

In Figure 3.3, the hexagonal cell's length of the inclined and non-inclined walls are shown as l_1 and h_1, respectively. Meanwhile, the cell angle and wall thickness are respectively defined by θ_1 and t_1 for hexagonal cell. For re-entrant hexagonal cell, the lengths of inclined and non-inclined walls are given as l_2 and h_2, respectively in Figure 3.3. Similarly, θ_2 and t_2 are defined and they represent the cell angle and wall thickness, respectively. Finally, the length between hexagonal and re-entrant cells are defined by h_3 and its thickness is t_3. While designing the AuxHex unit cell, the following relationship is taken into account for more elegant unit cell design:

$$l_1 \cos\theta_1 = l_2 \cos\theta_2 \tag{3.1}$$

3.2 Analytical Model of Mechanical Properties

To get the formulations of Young's modulus and yield stregnth for the AuxHex structure, the article named as "Mechanical properties and energy absorption capability of AuxHex structure under in-plane compression: Theoretical and experimental studies" [12] is utilized and derivation of these formulations are presented in upcoming subchapter. It is assumed that a uniform compressive load has been applied to the

AuxHex unit cell and the unit cell wall is treated as an Euler-Bernoulli beam, assuming no shear deformation and disregarding any axial extension or compression deformation [35,36]. Additionally, it is assumed that the material exhibits linear elastic behavior and the applied strain is small enough to prevent any major changes in the geometry of the structures [35].

3.2.1 Mechanical properties under compressive load

A uniform compressive force, acting in the x-direction, has been applied to a representative unit cell of the 2D hybrid structure (see Figure 3.4).

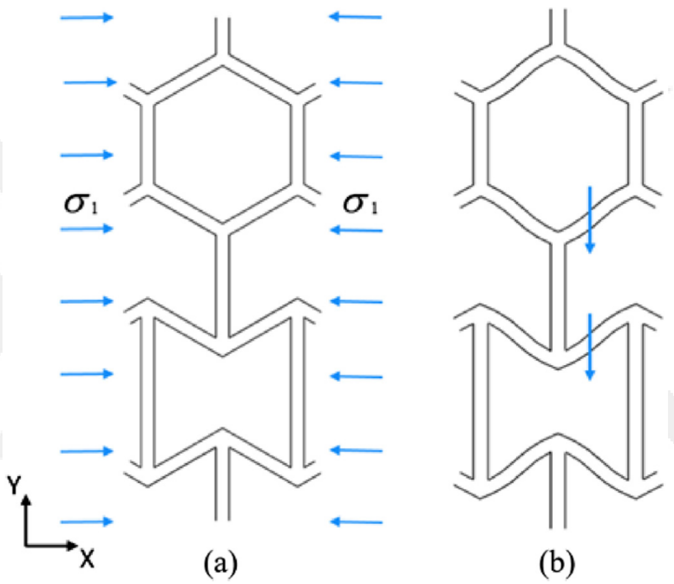

Figure 3.4 : (a) Loading in the x-direction and (b) predicted deformation [12].

Since both hexagonal and re-entrant hexagonal unit cells are expected to bend under load in x-direction as shown in Figure 3.4, force analysis was performed on both. However, based on the assumptions, only the inclined walls will exhibit significant bending. Therefore, taking advantage of symmetry, a single inclined wall for the force analysis can be isolated as shown in Figure 3.5.

In Figure 3.5, for beams AB and CD to be in equilibrium, there should not be any force acting in the y-direction. This allows to state the bending moment acting on beam AB as:

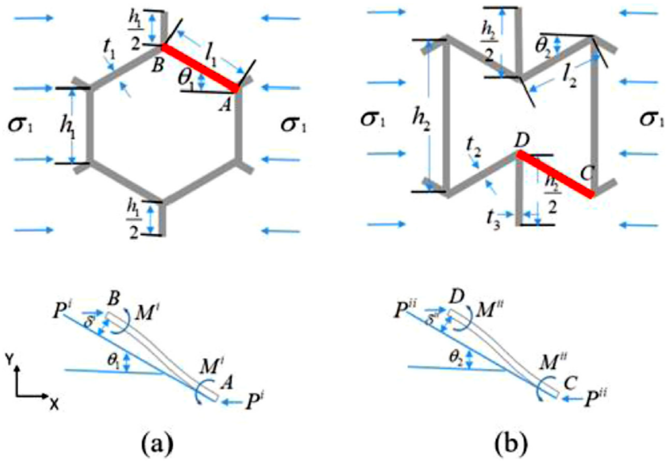

Figure 3.5 : Investigating the elastic response of (a) hexagonal and (b) re-entrant hexagonal cells under x-directional loading [12].

$$M_x^i = \frac{1}{2} P^i l_1 \sin\theta_1 \tag{3.2}$$

where P^i defines the force in the x-direction acting on beam AB. At this point, it should be noted that two superscripts i and ii reflect the hexagonal and re-entrant hexagonal cells, respectively. The force P^i is given as:

$$P^i = \frac{1}{2}\sigma_1 \left(2h_1 + 2l_1 sin\theta_1\right) b \tag{3.3}$$

The equation below describes the approximate deflection curve of the beam:

$$w'' = \frac{M(x)}{E_s I} \tag{3.4}$$

Beam AB's boundary conditions are given as:

$$Point\ A : w = 0,\ \theta \neq 0 \quad Point\ B : w \neq 0,\ \theta = 0 \tag{3.5}$$

From equations (3.4) and (3.5), beam AB's deflection can be yielded as:

$$\delta_x^i = \frac{M_x^i l_1^2}{6E_s I^i} \quad where \quad I^i = \frac{bt_1^3}{12} \tag{3.6}$$

where E_s is Young's modulus of the parent material and, where b refers to the length of the AuxHex unit cell through out-of-plane direction (z-direction).

The hexagonal cell's strain is expressed as below in the x-direction:

$$\varepsilon_x^i = \frac{\delta_x^i \sin\theta_1}{l_1 \cos\theta_1} = \frac{\sigma_1}{2E_s} \frac{(2h_1 + 2l_1 \sin\theta_1)\, l_1^2 \sin^2\theta_1}{t_1^3 \cos\theta_1} \tag{3.7}$$

Beam CD's bending moment is expressed by the equation:

$$M_x^{ii} = \frac{1}{2} P^{ii} l_2 \sin\theta_2 \tag{3.8}$$

where P^{ii} equals to the force of the beam CD in the x-direction.

$$P^{ii} = \frac{1}{2}\sigma_1 (2h_2 - 2l_2 \sin\theta_2)\, b \;\; if \;\; h_2 \geq 2l_2 \sin\theta_2, \;\; P^{ii} = \frac{1}{2}\sigma_1 h_2 b \;\; if \;\; h_2 < 2l_2 \sin\theta_2 \tag{3.9}$$

As beam AB having the boundary conditions, beam CD also has the same boundary conditions. Hence, beam CD's deflection equation is:

$$\delta_x^{ii} = \frac{M_x^{ii} l_2^2}{6E_s I^{ii}} \quad where \quad I^{ii} = \frac{bt_2^3}{12} \tag{3.10}$$

If the condition of $h_2 \geq 2l_2 sin\theta_2$ is maintained, further manipulation of Eq. (3.10) gives Eq. (3.11) as follows:

$$\delta_x^{ii} = \frac{\sigma_1 (2h_2 - 2l_2 sin\theta_2)\, bl_2^3 sin\theta_2}{24E_s I^{ii}} \tag{3.11}$$

The re-entrant hexagonal cell's the strain in the x-direction can be stated as:

$$\varepsilon_x^{ii} = \frac{\delta_x^{ii} sin\theta_2}{l_2 cos\theta_2} = \frac{\sigma_1}{2E_s} \frac{(2h_2 - 2l_2 sin\theta_2)\, l_2^2 sin^2\theta_2}{t_2^3 cos\theta_2} \tag{3.12}$$

2D hybrid cell's strain in the x-direction is obtained as:

$$\varepsilon_x = \frac{\sigma_1}{4E_s} \left[\frac{(2h_1 + 2l_1 sin\theta_1)}{t_1^3 cos\theta_1} l_1^2 sin^2\theta_1 + \frac{(h_2 - l_2 sin\theta_2)}{t_2^3 cos\theta_2} l_2^2 sin^2\theta_2 \right] \tag{3.13}$$

Moreover, Young's modulus through x-direction is expressed as:

$$E_1 = \frac{2E_s}{\left[\frac{(h_1+l_1 sin\theta_1)}{t_1^3 cos\theta_1} l_1^2 sin^2\theta_1 + \frac{(h_2-l_2 sin\theta_2)}{t_2^3 cos\theta_2} l_2^2 sin^2\theta_2\right]} \tag{3.14}$$

If the material of the cell wall reaches a plastic yield point, the structure will undergo plastic collapse once the bending moment equals to the plastic moment, thus establishing the plastic collapse stress of the structure. Likewise, unit cells are categorized into hexagonal and re-entrant hexagonal configurations for examination purposes.

For the hexagonal cell, an upper limit on the plastic collapse stress is given by equating the work done by the force P^i. The plastic work done at these four hinges (see Figure 3.6(a)) is given below:

$$4M_{1p}^i \phi^i \geq 2P^i l_1 \phi^i \sin\theta_1 \tag{3.15}$$

where M_{1p}^i is the bending wall's full plastic moment ($M_{1p}^i = \frac{1}{4}\sigma_y b t_1^2$ and where σ_y refers to the yield stress of the parent material.).

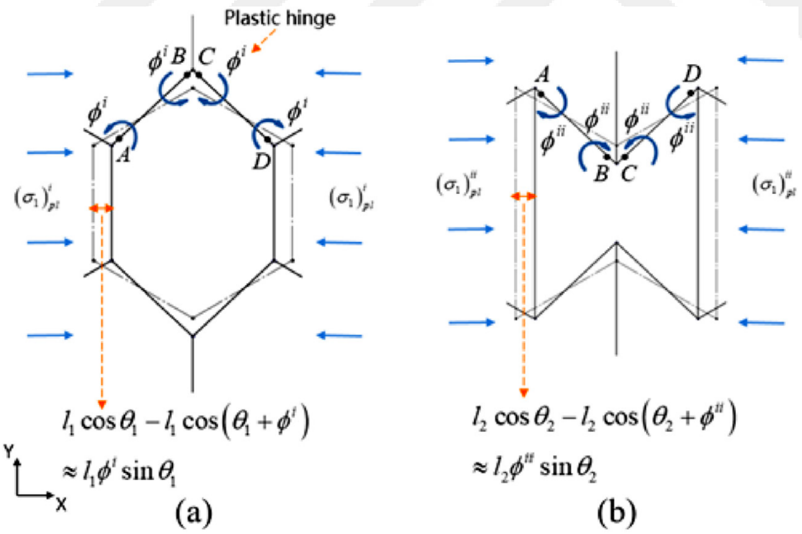

Figure 3.6 : Visualization of the deformation modes leading to plastic collapse in (a) hexagonal and (b) re-entrant hexagonal honeycombs subjected to x-directional loading [12].

Moreover, the plastic collapse stress's upper limit is found as:

$$(\sigma_1)_{pl}^i \leq \frac{\sigma_y t_1^2}{(2h_1 + 2l_1 sin\theta_1)\, l_1 sin\theta_1} \tag{3.16}$$

And, the lower limit of the plastic collpase stress can be found by equating the maximum moment in the beam to M^i_{1p}, which can be given as:

$$M^i_{1max} = \frac{1}{2}(\sigma_1)^i_{pl}(h_1 + l_!sin\theta_1)\,bl_1sin\theta_1 \tag{3.17}$$

From which, the upcoming formulation can be found out:

$$(\sigma_1)^i_{pl} \geq \frac{\sigma_y t_1^2}{(2h_1 + 2l_1 sin\theta_1)\,l_1 sin\theta_1} \tag{3.18}$$

It should be paid attention that both upper and lower limits are same. So, the hexagonal cell's plastic collapse stress is derived as:

$$(\sigma_1)^i_{pl} = \sigma_y \times \frac{t_1^2}{l_1^2} \times \frac{1}{2\,(h_1/l_1 + sin\theta_1)\,sin\theta_1} \tag{3.19}$$

Additionally, an upper limit on the plastic collapse stress is given by equating the work done by the force P^{ii} for the re-entrant hexagonal cell. As stated, the two results are same and the plastic collapse stress of the re-entrant hexagonal cell is obtained from the relationship below:

$$(\sigma_1)^{ii}_{pl} = \sigma_y \times \frac{t_2^2}{l_2^2} \times \frac{1}{2\,(h_2/l_2 - sin\theta_2)\,sin\theta_2} \tag{3.20}$$

The entire AuxHex structure will collapse plastically when either the hexagonal or re-entrant hexagonal cell reaches its own plastic collapse stress limit under the force in x-direction. So, the overall strength of the AuxHex structure in the x-direction is whichever of these two limits is lower.

3.3 FEM Simulation of Lattice Structure of AuxHex

Within the scope of this study, the ABAQUS 2020 finite element program [37] with explicit solver was employed to investigate the influence of varying design parameters on the mechanical properties of the structure. In the finite element model, the bottom plate of the core structure was constrained in all directions. The top plate was subjected to an axial compressive displacement until 0.75 mm/mm strain, while the remaining directions of the bottom plate were constrained. The nylon material used in the study, named as PA2200, has a density of 930 kg/m^3 [38] and a Poisson's ratio of 0.395 [39]. For a thickness of 0.55 mm, the stress-strain curve defining the material properties was digitized from the article [12] and imported into the ABAQUS finite element program. The digitized stress-strain curve for the corresponding material is as shown in Figure 3.7. The PA2200 material exhibited a Young's modulus of 908 MPa and a yield strength of 16 MPa at a thickness of 0.55 mm.

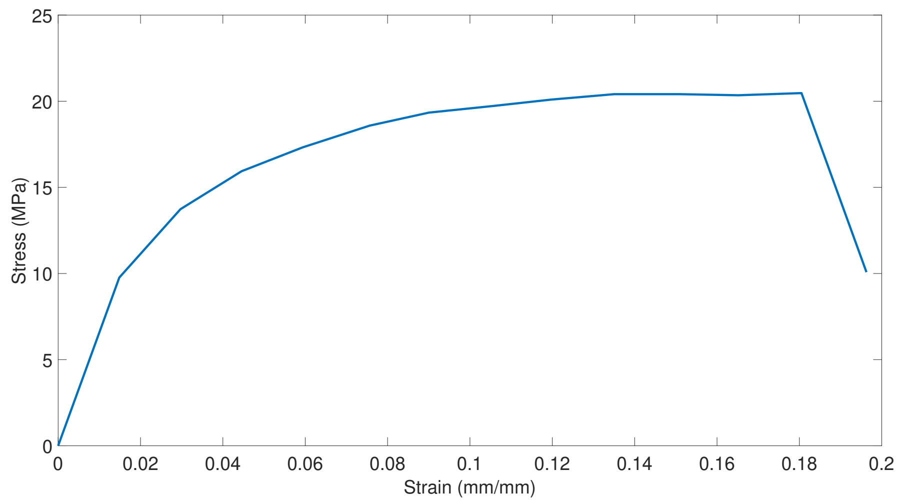

Figure 3.7 : The stress-strain curve from the tensile test of PA2200.

For further investigation of AuxHex's mechanical properties with various design parameters, the article [12] from the literature was selected to do benchmarking and verify the FEM models. Accordingly, the thicknesses of the top and bottom plates were set to 1.00 mm, while the design parameters of the AuxHex unit cells are presented in Table 3.1.

Table 3.1 : Design parameters for AuxHex unit cell.

Structure	l_1 (mm)	h_1 (mm)	t_1 (mm)	θ_1 (degree)	l_2 (mm)
AuxHex	5	5	0.55	30	5
Structure	**h_2 (mm)**	**t_2 (mm)**	**θ_2 (degree)**	**h_3 (mm)**	**t_3 (mm)**
AuxHex	10	0.55	30	7.5	0.55

For the AuxHex sandwich structure, the ABAQUS finite element program was employed to construct a two-dimensional model using S4R-type quadrilateral shell elements with reduced integration and hourglass control. The objective was to solve the model as quickly as possible using two-dimensional elements with high accuracy [18,26,40]. Hard contact was defined on the FEM model to simulate interaction of unit cells with each other. The force-displacement data obtained from the top plate of the AuxHex sandwich structure was converted to the stress-strain data so as to compare the results with the mentioned article.

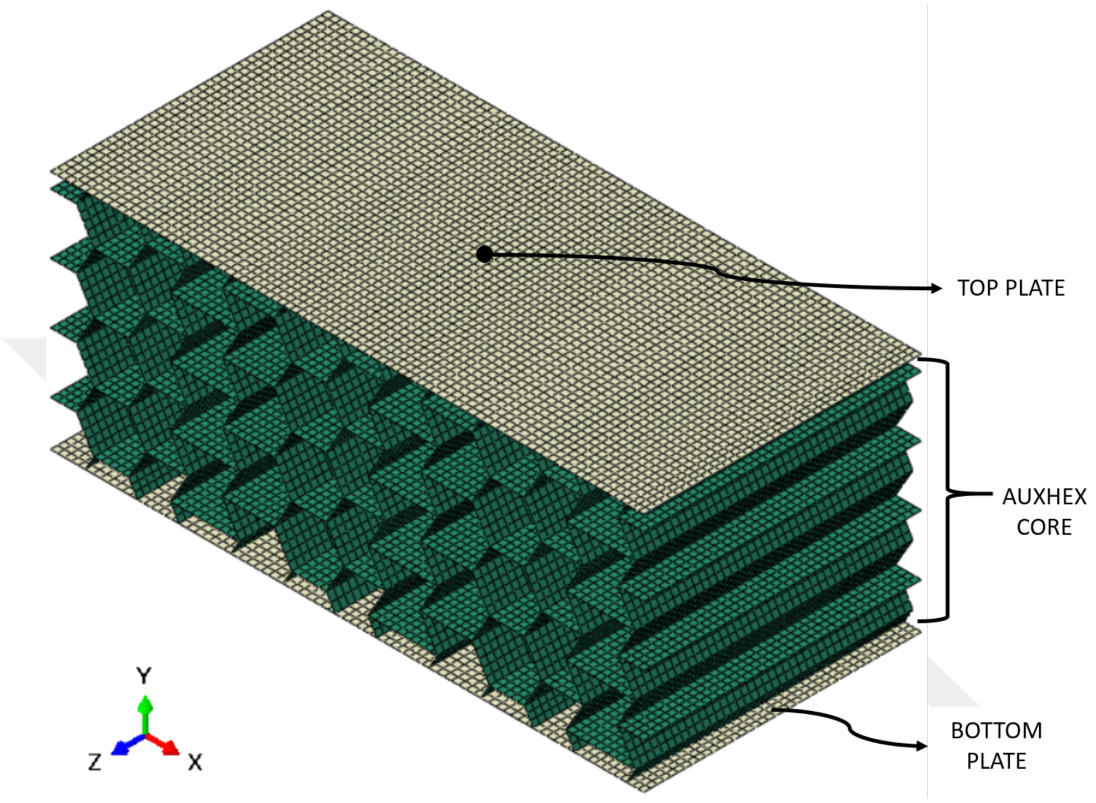

Figure 3.8 : FEM Model.

The comparison of the obtained results with the reference study [12] in terms of stress-strain is shown in the Figure 3.9. This comparison demonstrates that close results were obtained, validating the FEM model for further analyses.

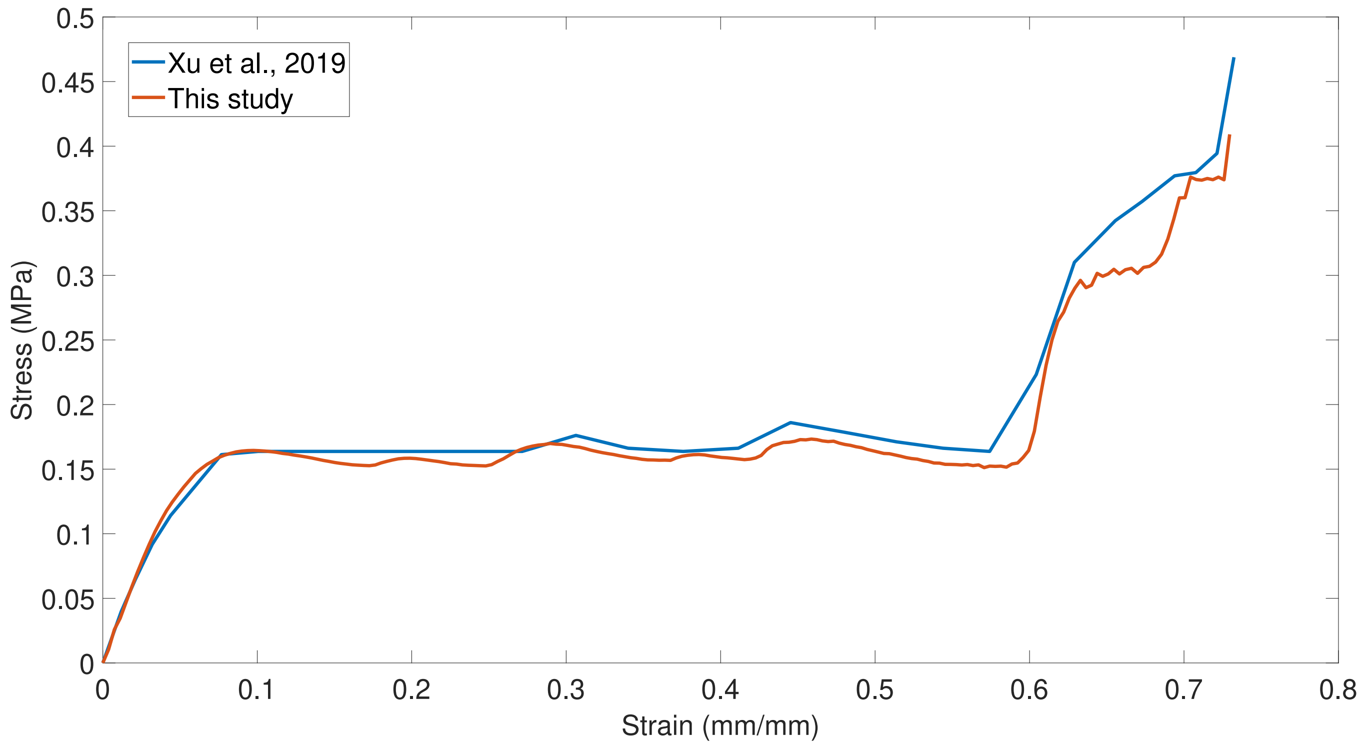

Figure 3.9 : Validation study in terms of stress-strain.

4. MODELING, SIMULATION, AND RESULTS

In this chapter, mechanical properties of various design parameters of AuxHex core structure is obtained. The mechanical properties investigated include the Young modulus, yield strength, and energy absorption values at 10% and 25% of strain and toughness of AuxHex core structure.

4.1 Design Parameters of AuxHex Unit Cells

This section outlines the design assumptions and parameters employed to investigate the AuxHex structure. The AuxHex unit cell structure is depicted in Figure 3.3. The following assumptions are made regarding the design parameters defining the unit cell shown in Figure 3.3:

1) $h = h_1 = h_2/2 = h_3$

2) $l = l_1 = l_2$

3) $\theta = \theta_1 = \theta_2$

4) $t = t_1 = t_2 = t_3$

Under the assumpitons made above, the parameters h and l will take values between 5 and 10 mm with an increment of 2.5 mm, while θ will be varied from 20° to 40° with increments of 10°. The thickness value (t) will be increased from 0.4 mm to 0.6 mm with increments of 0.1 mm. The increments and limits of each design parameter are uniquely determined without referencing any other examples. To facilitate evaluation based on the results, a coding scheme has been developed for the structures that will emerge with different design parameters. For instance, when $h = h_1 = h_2/2 = h_3 = 7.5\,mm$, $l = l_1 = l_2 = 7.5\,mm$, $\theta = \theta_1 = \theta_2 = 30°$ and $t = t_1 = t_2 = t_3 = 0.5\,mm$ are introduced on the unit cell of AuxHex, this design is coded as *H7.5-L7.5-TH30-T0.5*. All codes and related design parameters are listed in Table 4.1.

Table 4.1 : Codes and design parameters for each investigated unit cells.

Codes	h (mm)	l (mm)	θ (°)	t (mm)
H7.5-L7.5-TH30-T0.5	7.5	7.5	30	0.5
H5-L7.5-TH30-T0.5	5	7.5	30	0.5
H10-L7.5-TH30-T0.5	10	7.5	30	0.5
H7.5-L5-TH30-T0.5	7.5	5	30	0.5
H7.5-L10-TH30-T0.5	7.5	10	30	0.5
H7.5-L7.5-TH20-T0.5	7.5	10	20	0.5
H7.5-L7.5-TH40-T0.5	7.5	10	40	0.5
H7.5-L7.5-TH30-T0.4	7.5	10	30	0.4
H7.5-L7.5-TH30-T0.6	7.5	10	30	0.6

4.1.1 Geometric dimensions of AuxHex specimens

In this subsection, the detailed breakdown of the cell's structural parameters and the geometric dimensions of the AuxHex core panels is provided in Table 4.2. Number of unit cell which is 3x4 for each specific design means that there are a total of 3 unit cells through length and 4 unit cells through width. For each AuxHex structures listed in Table 4.1, depth is taken as 40 mm. Directions of height (H), width (W) and depth (D) are shown in Figure 4.1.

Table 4.2 : Geometric dimensions of AuxHex core structures with codes.

Codes	Height (mm)	Width (mm)
H7.5-L7.5-TH30-T0.5	51.96	116.25
H5-L7.5-TH30-T0.5	51.96	77.5
H10-L7.5-TH30-T0.5	51.96	155
H7.5-L5-TH30-T0.5	34.64	116.25
H7.5-L10-TH30-T0.5	69.28	116.25
H7.5-L7.5-TH20-T0.5	56.38	116.25
H7.5-L7.5-TH40-T0.5	45.96	112.5
H7.5-L7.5-TH30-T0.4	51.96	116.25
H7.5-L7.5-TH30-T0.6	51.96	116.25

4.2 Investigation of Mechanical Properties

Herein, it is aimed to see the effects of different design parameters on the mechanical properties of AuxHex core structure. In the following first subsection, the influence of varying design parameters on the structure's Young's modulus and yield strength is

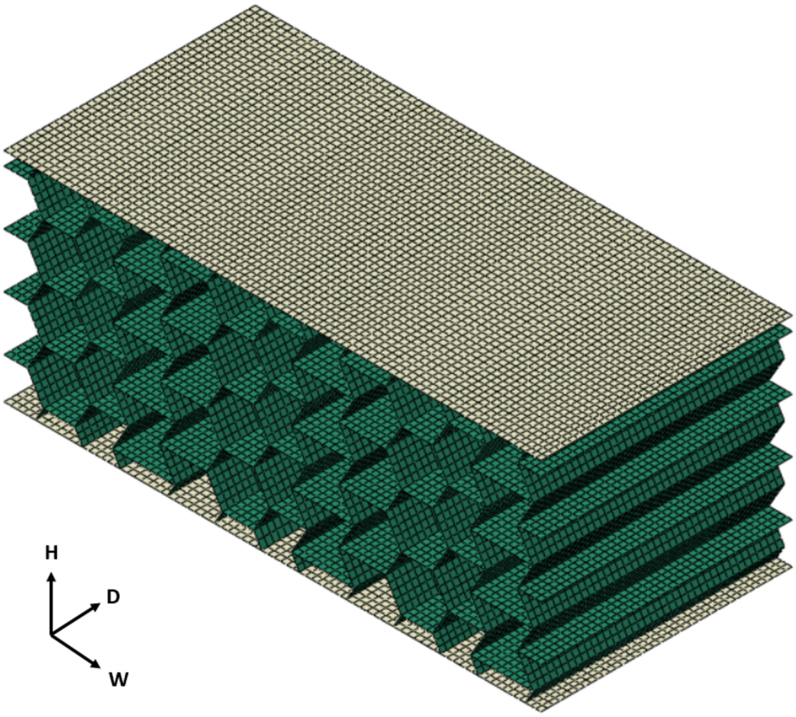

Figure 4.1 : H-D-W directions for geometric dimensions of AuxHex core structure.

investigated by using both theoretical formulas and FEM model results. Chapter 4.2.2 presents the effect of changing design parameters on the structure's energy absorption capability and toughness. All Young's modulus, yield strength, energy absorption capability and toughness values are calculated specifically which means all results are divided by related AuxHex structure's mass.

4.2.1 Young's modulus and yield strength

To calculate theoretically the Young's modulus and yield strength of AuxHex core structure, it is better to recall the Eqs. 3.14, 3.19 and 3.20 from Chapter 3.2.1:

Young's modulus:

$$E_1 = \frac{2E_s}{\left[\frac{(h_1+l_1 sin\theta_1)}{t_1^3 cos\theta_1} l_1^2 sin^2\theta_1 + \frac{(h_2-l_2 sin\theta_2)}{t_2^3 cos\theta_2} l_2^2 sin^2\theta_2\right]} \tag{4.1}$$

Yield strength for conventional hexagonal cell:

$$(\sigma_1)_{pl}^i = \sigma_y \times \frac{t_1^2}{l_1^2} \times \frac{1}{2\left(h_1/l_1 + sin\theta_1\right) sin\theta_1} \tag{4.2}$$

Yield strength for re-entrant hexagonal cell:

$$(\sigma_1)_{pl}^{ii} = \sigma_y \times \frac{t_2^2}{l_2^2} \times \frac{1}{2\,(h_2/l_2 - sin\theta_2)\,sin\theta_2} \tag{4.3}$$

Again, it should be noted that the entire AuxHex structure will collapse plastically when either the hexagonal or re-entrant hexagonal cell reaches its own plastic collapse stress limit under the force in x-direction. So, the overall strength of the AuxHex structure in the x-direction is whichever of these two limits is lower.

4.2.1.1 Effect of the length of non-inclined wall (*h*)

The AuxHex structures coded as **H5**-L7.5-TH30-T0.5, **H7.5**-L7.5-TH30-T0.5, **H10**-L7.5-TH30-T0.5 are investigated here to observe the effect of a longer non-inclined wall length (h) on AuxHex structures. It's worth mentioning that only h takes values 5, 7.5, and 10 mm while other design parameters l, θ, and t are kept as-is.

With increased non-inclined wall length (h), the Young's modulus and yield strength results from the formulations and FEM results are tabulated in Table 4.3 and Table 4.4, respectively.

Table 4.3 : Specific theoretical and FEM results for Young's modulus with increased non-inclined wall length (h).

E (MPa/kg)	**H5**-L7.5-TH30-T0.5	**H7.5**-L7.5-TH30-T0.5	**H10**-L7.5-TH30-T0.5
Theoretical	38.671	21.133	13.390
FEM	39.241	21.187	13.075

Table 4.4 : Specific theoretical and FEM results for yield strength with increased non-inclined wall length (h).

YS (MPa/kg)	**H5**-L7.5-TH30-T0.5	**H7.5**-L7.5-TH30-T0.5	**H10**-L7.5-TH30-T0.5
Theoretical	2.529	1.612	1.115
FEM	2.477	1.300	0.901

The tables above proves that both E and YS decrease when the length of non-inclined walls (h) increases.

The differences between theoretical and FEM results are previously obtained in the literature [12]. The observed discrepancies may be caused by two factors: the inherent limitations of using discretized sizes to represent continuous geometries, and the uncertainties associated with the material properties of complex structures.

4.2.1.2 Effect of the length of inclined wall (*l*)

The AuxHex structures coded as H7.5-**L5**-TH30-T0.5, H7.5-**L7.5**-TH30-T0.5, H7.5-**L10**-TH30-T0.5 are investigated here to observe the effect of a longer inclined wall length (*l*) on AuxHex structures. It should be noted that only *l* takes values 5, 7.5, and 10 mm while other design parameters *h, θ,* and *t* are kept as-is.

With increased inclined wall length (*l*), the Young's modulus and yield strength results from the formulations and FEM results are tabulated in Table 4.5 and Table 4.6, respectively.

Table 4.5 : Specific theoretical and FEM results for Young's modulus with increased inclined wall length (*l*).

E (MPa/kg)	H7.5-**L5**-TH30-T0.5	H7.5-**L7.5**-TH30-T0.5	H7.5-**L10**-TH30-T0.5
Theoretical	55.918	21.133	10.309
FEM	55.800	21.187	9.938

Table 4.6 : Specific theoretical and FEM results for yield strength with increased inclined wall length (*l*).

YS (MPa/kg)	H7.5-**L5**-TH30-T0.5	H7.5-**L7.5**-TH30-T0.5	H7.5-**L10**-TH30-T0.5
Theoretical	3.200	1.612	0.944
FEM	2.812	1.300	0.791

From Table 4.5 and 4.6, one can easily summarize the fact that when the inclined wall length of AuxHex unit cells increases, both E and YS values of the core structure decreases.

4.2.1.3 Effect of the unit cell's angle (θ)

The AuxHex structures coded as H7.5-L7.5-**TH20**-T0.5, H7.5-L7.5-**TH30**-T0.5, H7.5-L7.5-**TH40**-T0.5 are investigated here to observe the effect of the unit cell's angle (θ) on AuxHex structures. Importantly, only the parameter θ is varied, taking values of 20°, 30°, and 40° while other design parameters *h, l,* and *t* are kept as-is.

With increased angle of unit cell (θ), the Young's modulus and yield strength results from the formulations and FEM results are tabulated in Table 4.7 and Table 4.8, respectively.

Table 4.7 : Specific theoretical and FEM results for Young's modulus with increased unit cell's angle (θ).

E (MPa/kg)	H7.5-L7.5-**TH20**-T0.5	H7.5-L7.5-**TH30**-T0.5	H7.5-L7.5-**TH40**-T0.5
Theoretical	49.007	21.133	11.506
FEM	44.714	21.187	13.055

Table 4.8 : Specific theoretical and FEM results for yield strength with increased unit cell's angle (θ).

YS (MPa/kg)	H7.5-L7.5-**TH20**-T0.5	H7.5-L7.5-**TH30**-T0.5	H7.5-L7.5-**TH40**-T0.5
Theoretical	2.635	1.612	1.165
FEM	1.555	1.300	1.211

Tables 4.7 and 4.8 show that both E and YS decrease when the angle of unit cell (θ) increases.

4.2.1.4 Effect of the thickness of unit cell's wall (*t*)

The AuxHex structures coded as H7.5-L7.5-TH30-**T0.4**, H7.5-L7.5-TH30-**T0.5**, H7.5-L7.5-TH30-**T0.6** are investigated here to observe the effect of thicker walls of unit cell (t) on AuxHex structures. It is crucial to note that among all design parameters, only t undergoes changes, assuming values of 0.4, 0.5, and 0.6 mm, while h, l, and θ are held constant.

With increased thickness of unit cell's wall (t), the Young's modulus and yield strength results from the formulations and FEM results are tabulated in Table 4.9 and Table 4.10, respectively.

Table 4.9 : Specific theoretical and FEM results for Young's modulus with increased unit cell's wall thickness (t).

E (MPa/kg)	H7.5-L7.5-TH30-**T0.4**	H7.5-L7.5-TH30-**T0.5**	H7.5-L7.5-TH30-**T0.6**
Theoretical	12.574	21.133	31.953
FEM	11.818	21.187	31.765

The results summarized in Tables 4.9 and 4.10 show consistency between increased wall thickness and increased mechanical properties [41].

Table 4.10 : Specific theoretical and FEM results for yield strength with increased unit cell's wall thickness (t).

YS (MPa/kg)	H7.5-L7.5-TH30-**T0.4**	H7.5-L7.5-TH30-**T0.5**	H7.5-L7.5-TH30-**T0.6**
Theoretical	1.199	1.612	2.032
FEM	0.987	1.300	1.839

4.2.2 Energy absorption capability and toughness

The energy absorption (EA) capability at some certain values of strain and toughness of total 9 different AuxHex structure is discussed in this section. There is no direct formulation to obtain EA and toughness by using design parameters of unit cell like done for Young's modulus and yield strength. For this reason, force-displacement values from the top plates of each 9 different AuxHex structure's FEM model is obtained and converted to stress-strain graph to use the equations below:

$$EA_{0.1} = \int_0^{0.1} \sigma d\varepsilon \tag{4.4}$$

$$EA_{0.25} = \int_0^{0.25} \sigma d\varepsilon \tag{4.5}$$

$$Toughness = \int_0^{0.75} \sigma d\varepsilon \tag{4.6}$$

To provide a more detailed explanation of the meaning of the above equations 4.4, 4.5, and 4.6, these all 3 equations gives the area under stress-strain curve. The main discrepancy among these formulations is upper and lower boundaries of integrals. Eq. 4.4 is written for obtaining the energy absorption until $\varepsilon = 0.1\,mm/mm$ while Eq. 4.5 gives the absorbed energy until $\varepsilon = 0.25\,mm/mm$. Lastly, the toughness of each AuxHex model is calculated by taking integral of Eq. 4.6 since all FEM models are simulated until $\varepsilon = 0.75\,mm/mm$. The commercial software MATLAB [42] is utilized to find the results of integrals (Eqs. 4.4, 4.5, and 4.6) by doing curve fitting of stress-strain graphs.

4.2.2.1 Effect of the length of non-inclined wall (*h*)

Like done in previous chapter for getting E and YS values, the AuxHex structures coded as **H5**-L7.5-TH30-T0.5, **H7.5**-L7.5-TH30-T0.5, **H10**-L7.5-TH30-T0.5 are investigated here to observe the effect of a longer non-inclined wall length (*h*) on AuxHex structures' energy absorption capability. It's worth mentioning that only *h* take values 5, 7.5 and 10 mm while other design parameters *l*, θ, and *t* are kept as-is.

With increased non-inclined wall length (h), energy absorptions at 10% and 25% of strain and toughness are obtained from the stress-strain graphs of FEM results are tabulated in Table 4.11.

Table 4.11 : Specific energy absorption and toughness results for increased non-inclined wall length (*h*).

Unit Cell Structure	$EA_{0.1}$	$EA_{0.25}$	Toughness
H5-L7.5-TH30-T0.5	192.158	702.905	2760.166
H7.5-L7.5-TH30-T0.5	104.388	380.272	1350.340
H10-L7.5-TH30-T0.5	63.362	238.937	867.241

All EA and toughness results are in the unit of kJ/m^3kg.

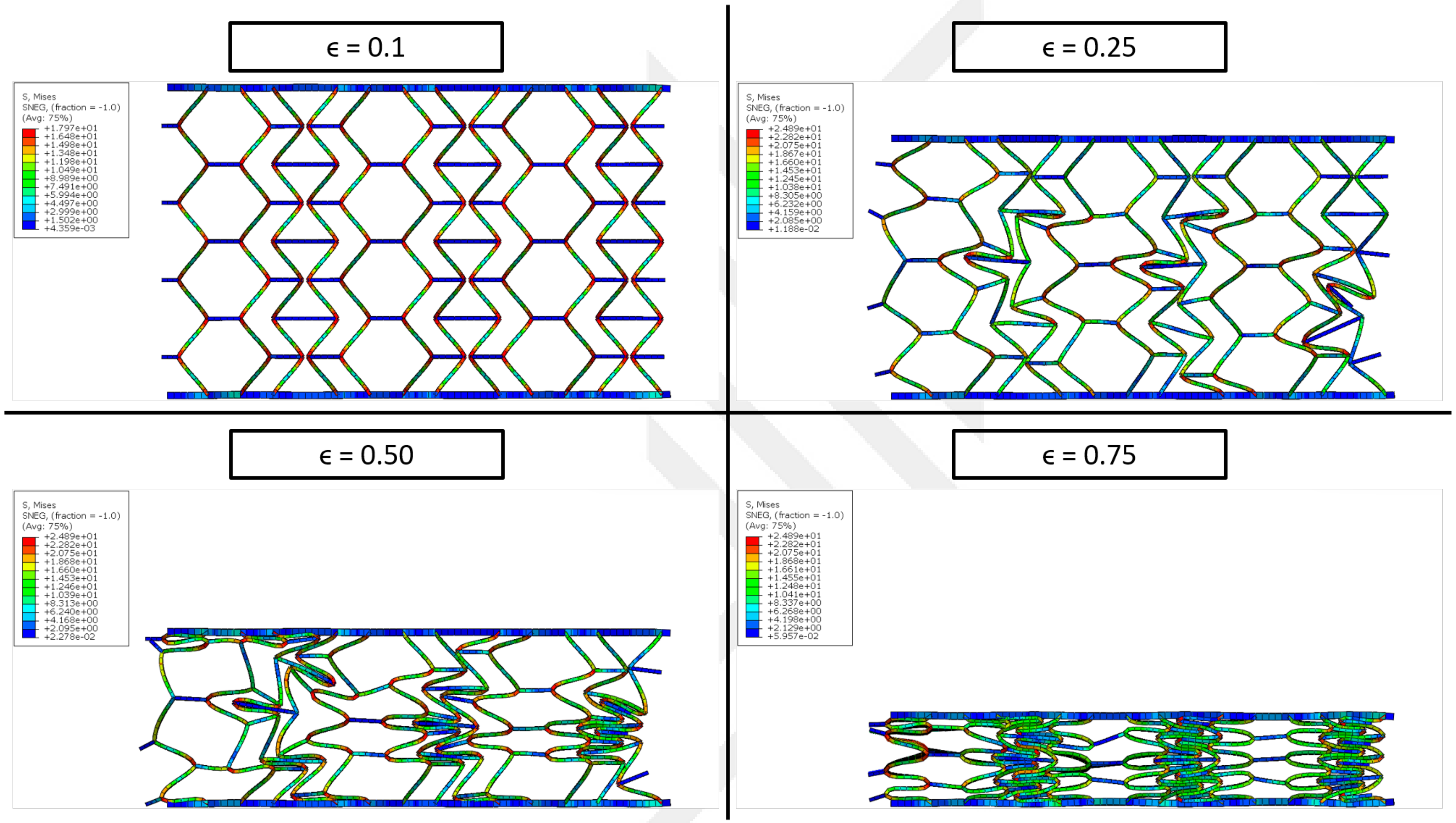

Figure 4.2 : Deformation modes of H5-L7.5-TH30-T0.5.

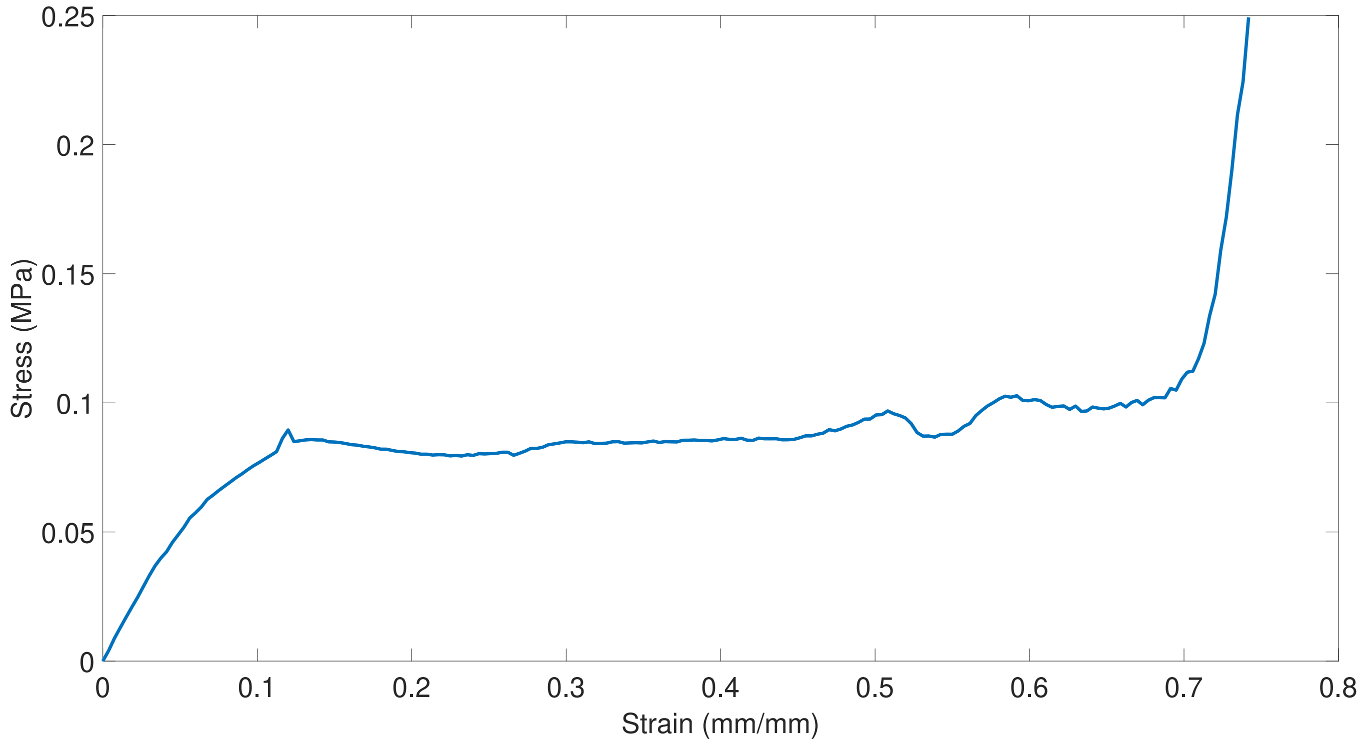

Figure 4.3 : Stress-strain graph of H5-L7.5-TH30-T0.5.

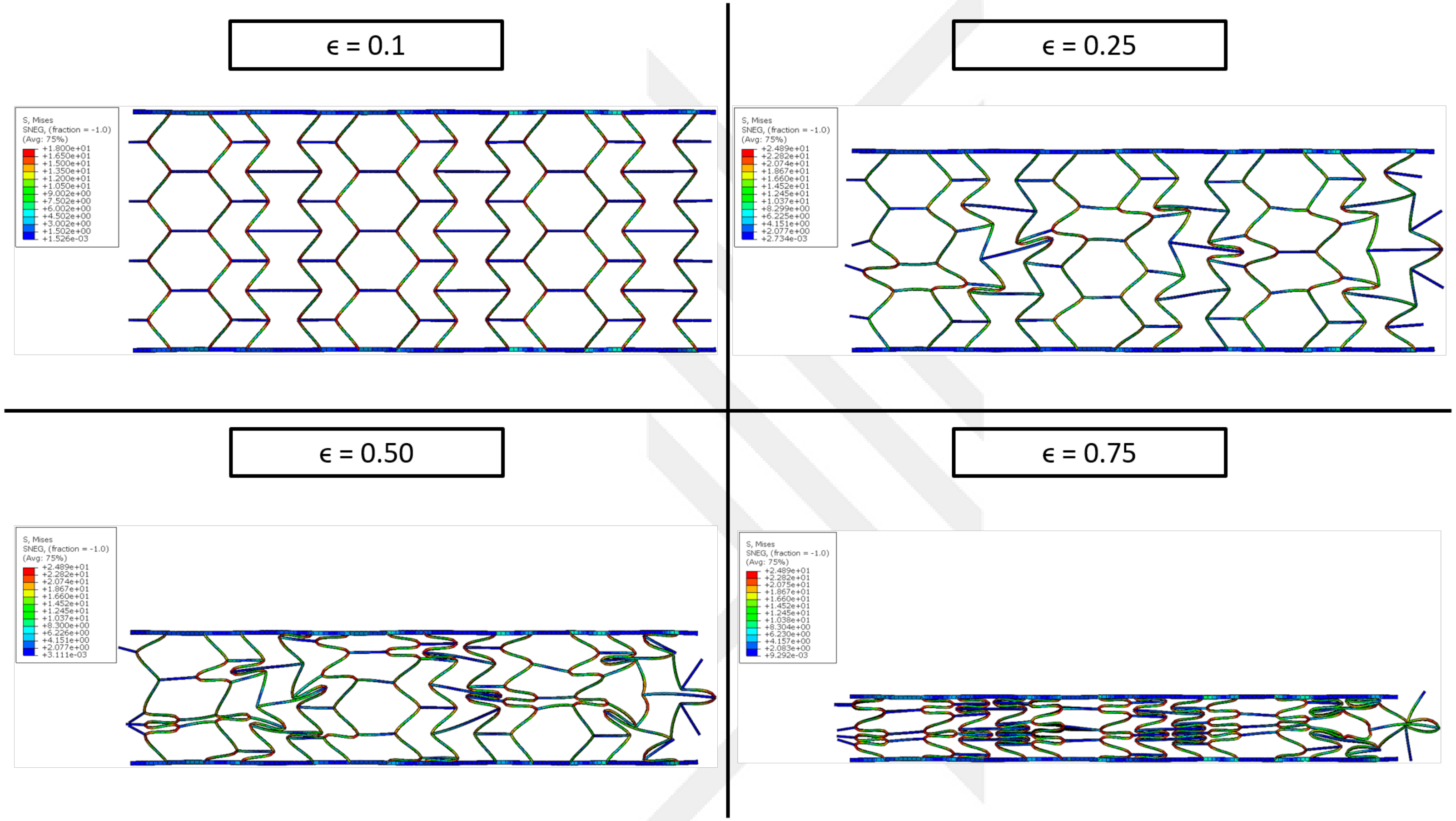

Figure 4.4 : Deformation modes of H7.5-L7.5-TH30-T0.5.

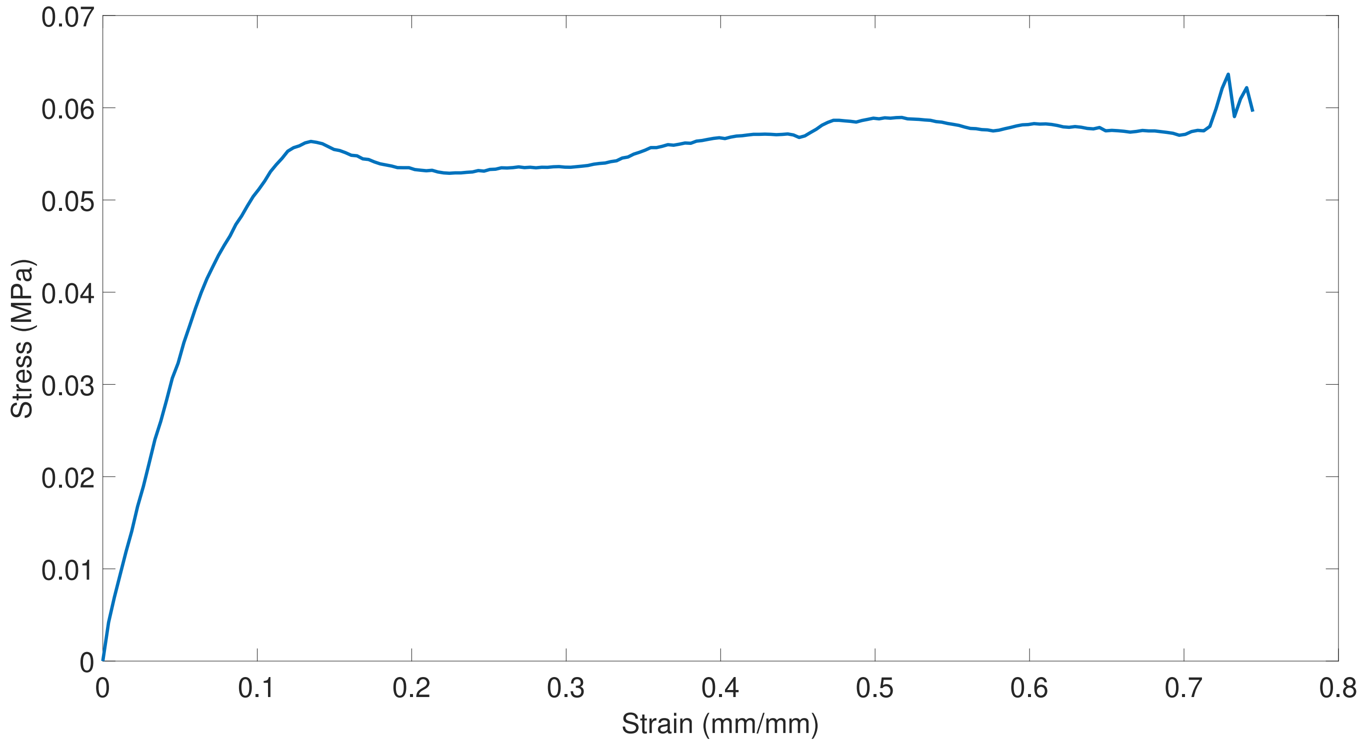

Figure 4.5 : Stress-strain graph of H7.5-L7.5-TH30-T0.5.

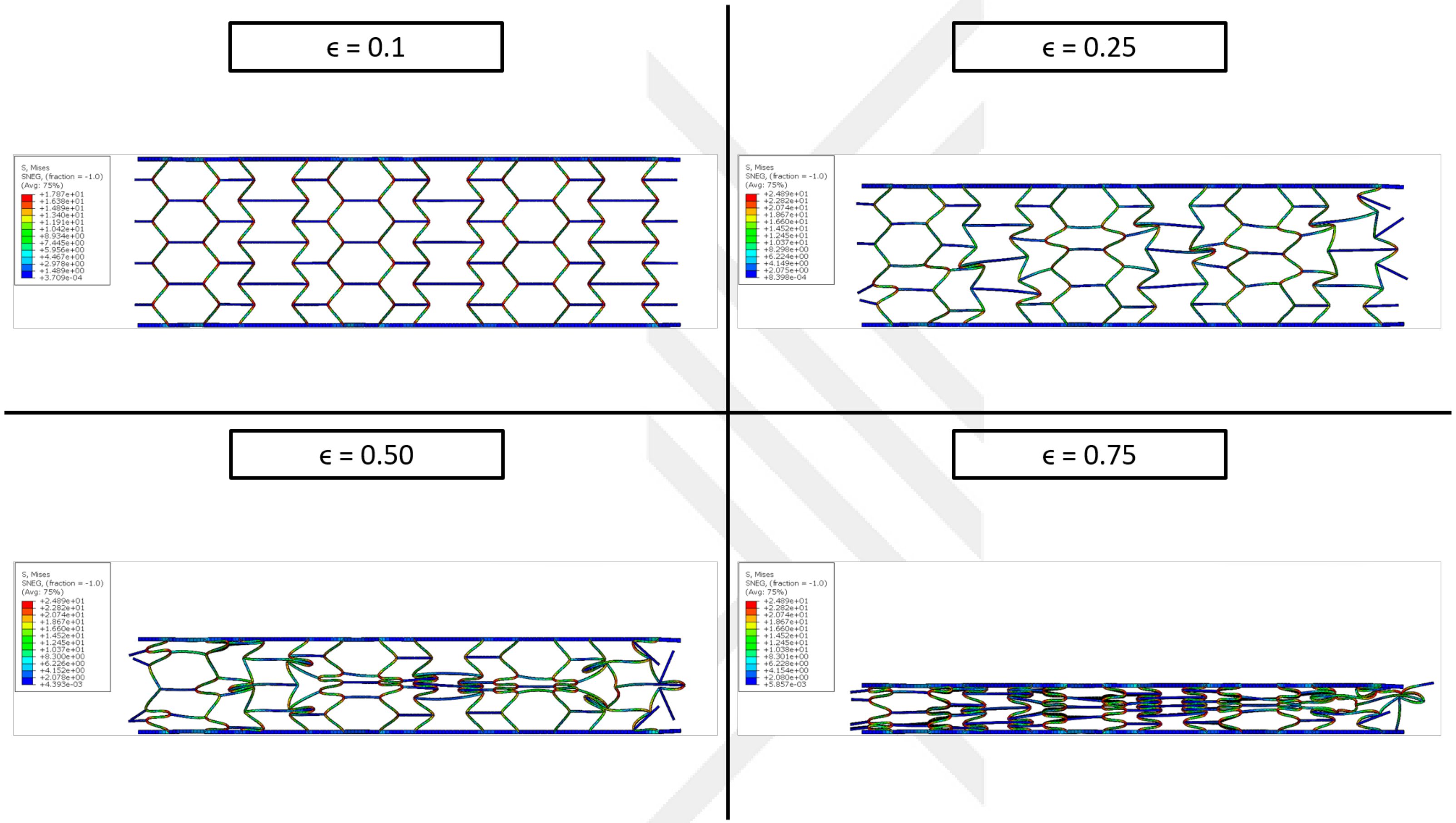

Figure 4.6 : Deformation modes of H10-L7.5-TH30-T0.5.

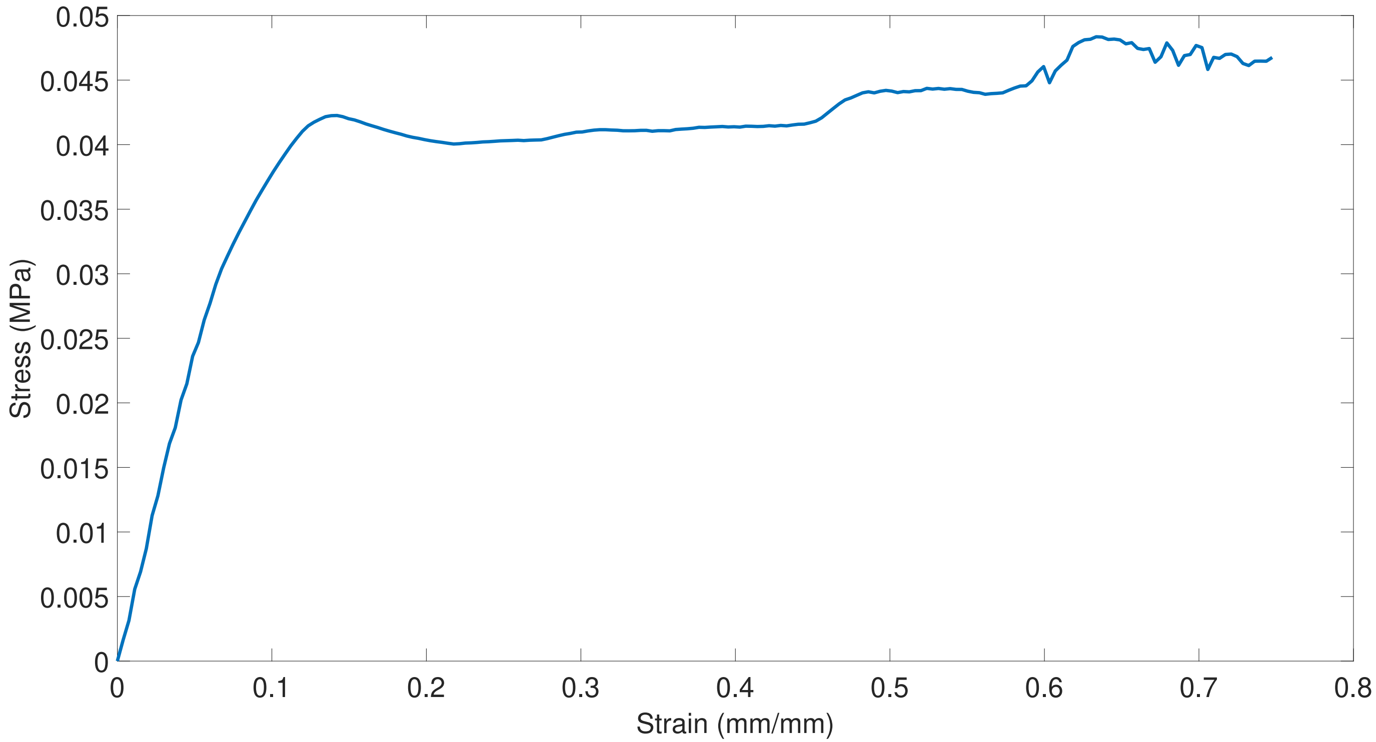

Figure 4.7 : Stress-strain graph of H10-L7.5-TH30-T0.5.

4.2.2.2 Effect of the length of inclined wall (*l*)

Like done in previous chapter for getting E and YS values, the AuxHex structures coded as H7.5-**L5**-TH30-T0.5, H7.5-**L7.5**-TH30-T0.5, H7.5-**L10**-TH30-T0.5 are investigated here to observe the effect of a longer inclined wall length (*l*) on AuxHex structures' energy absorption capability. It should be noted that only *l* takes values 5, 7.5, and 10 mm while other design parameters *h*, θ, and *t* are kept as-is.

With increased inclined wall length (*l*), energy absorptions at 10% and 25% of strain and toughness are obtained from the stress-strain graphs of FEM results are tabulated in Table 4.12.

Table 4.12 : Specific energy absorption and toughness results for increased inclined wall length (*l*).

Unit Cell Structure	$EA_{0.1}$	$EA_{0.25}$	Toughness
H7.5-**L5**-TH30-T0.5	241.360	808.800	2799.200
H7.5-**L7.5**-TH30-T0.5	104.388	380.272	1350.340
H7.5-**L10**-TH30-T0.5	52.389	209.204	809.735

All EA and toughness results are in the unit of kJ/m^3kg.

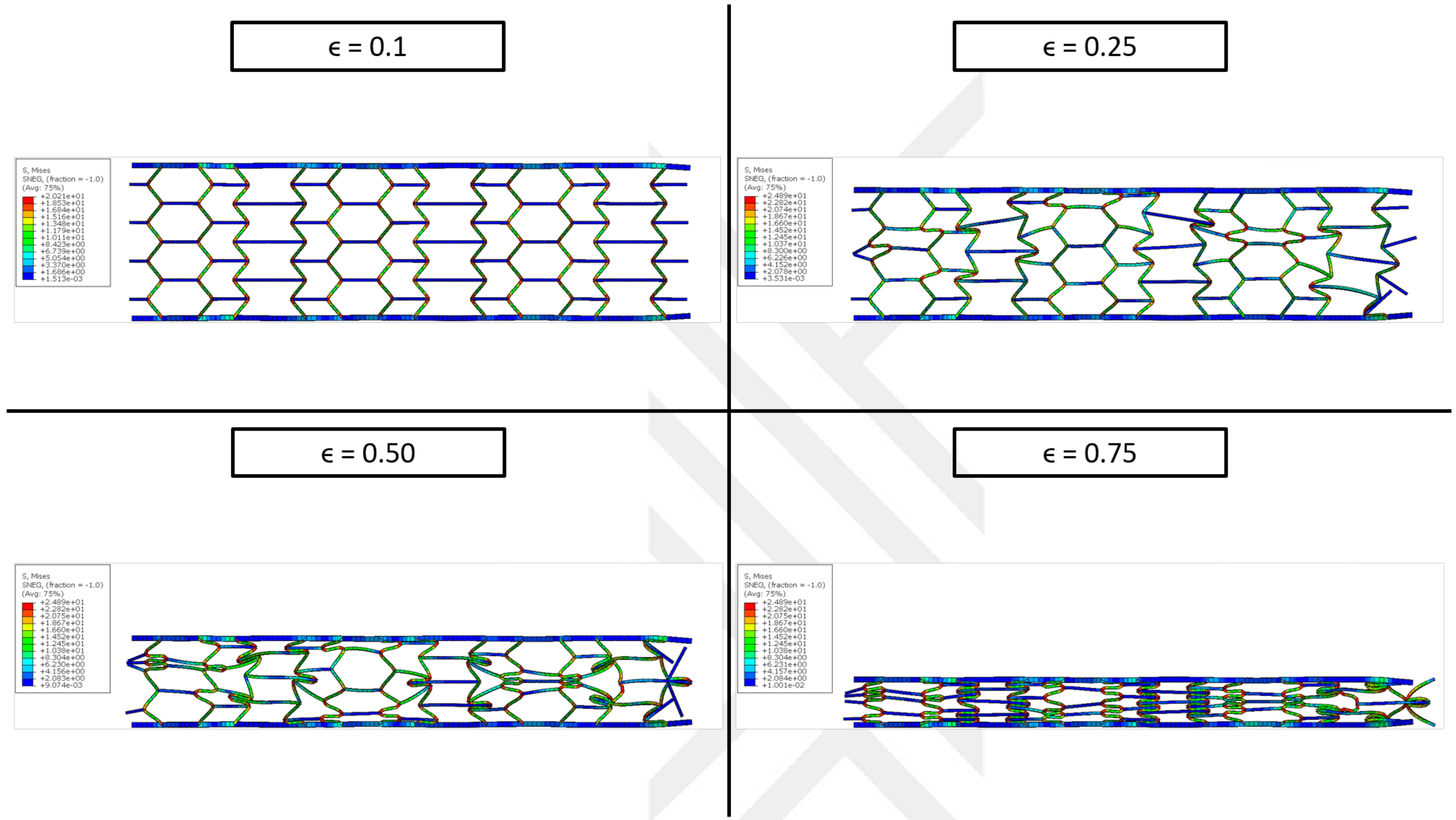

Figure 4.8 : Deformation modes of H7.5-L5-TH30-T0.5.

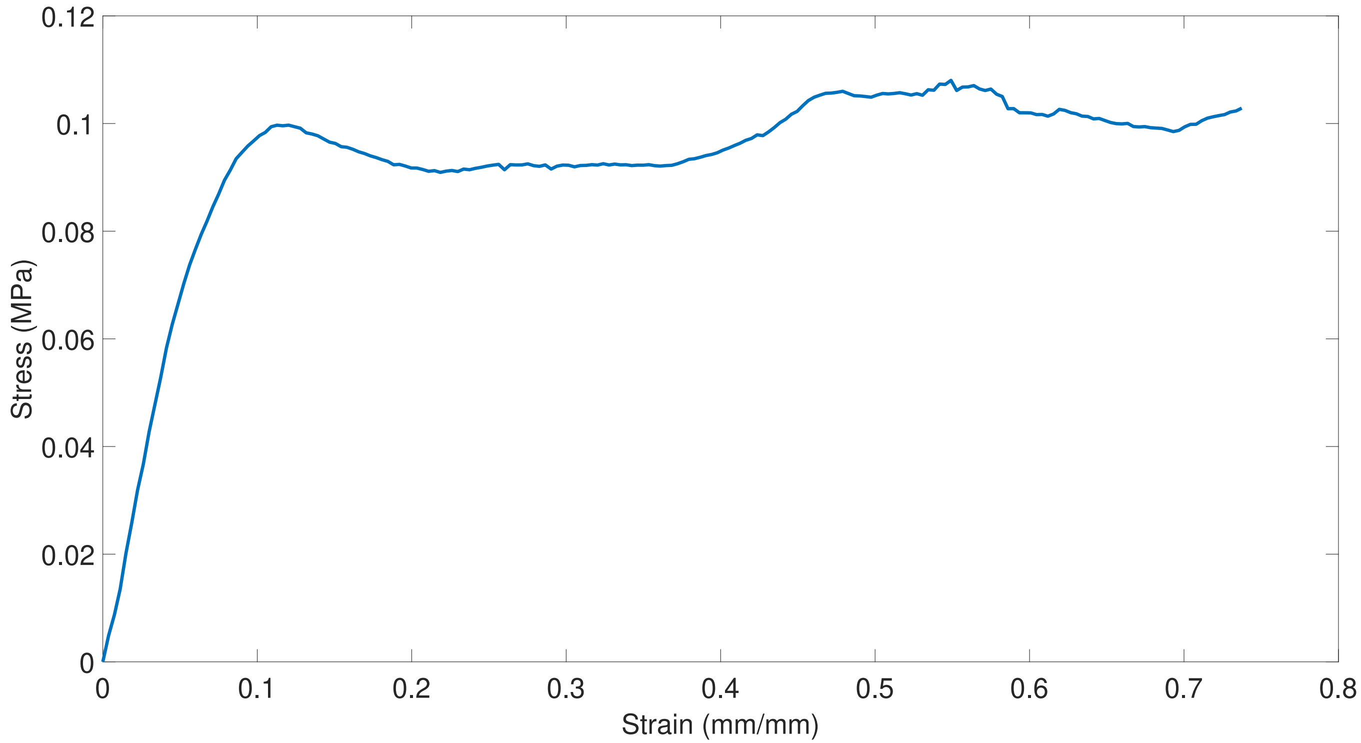

Figure 4.9 : Stress-strain graph of H7.5-L5-TH30-T0.5.

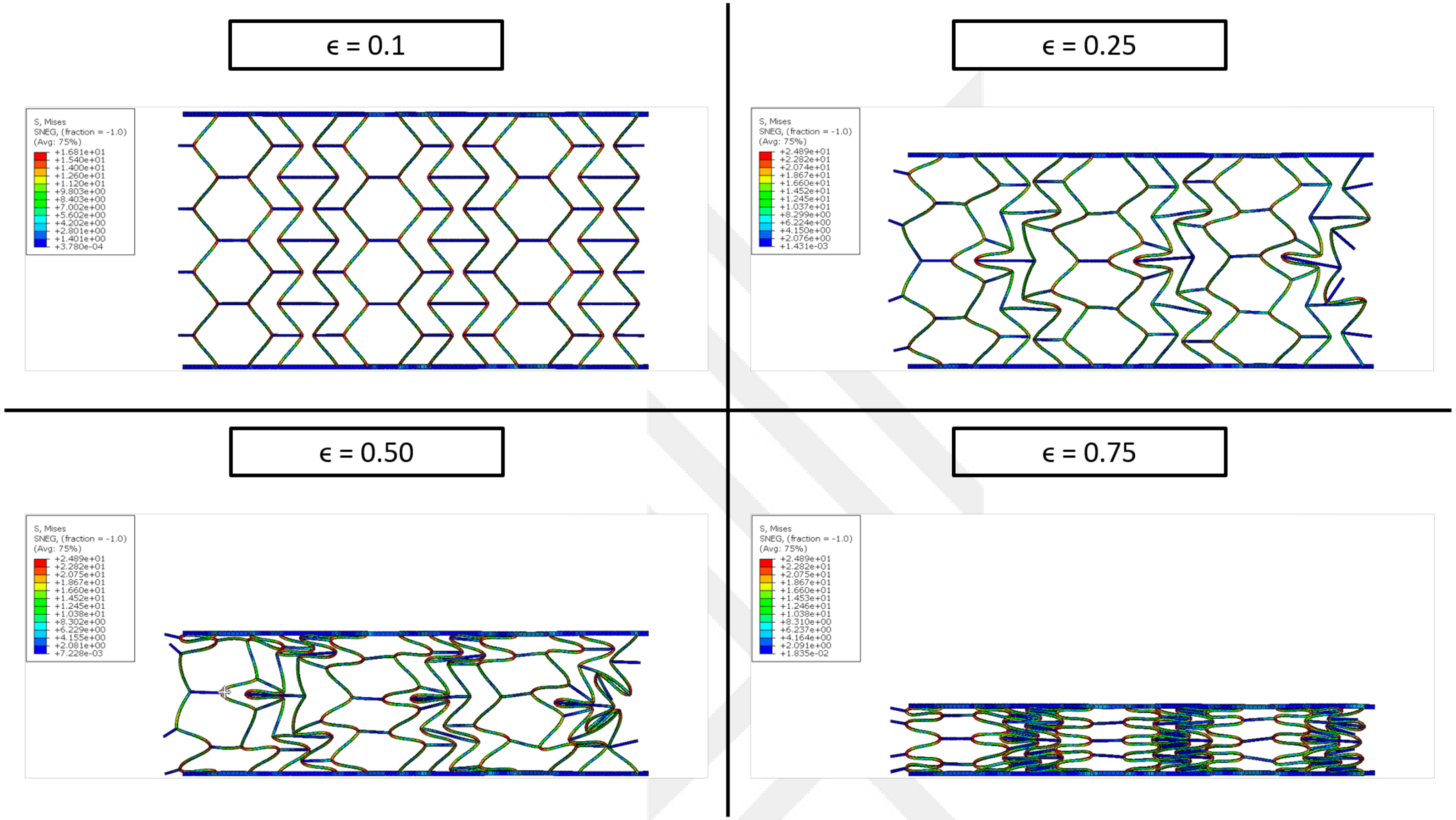

Figure 4.10 : Deformation modes of H7.5-L10-TH30-T0.5.

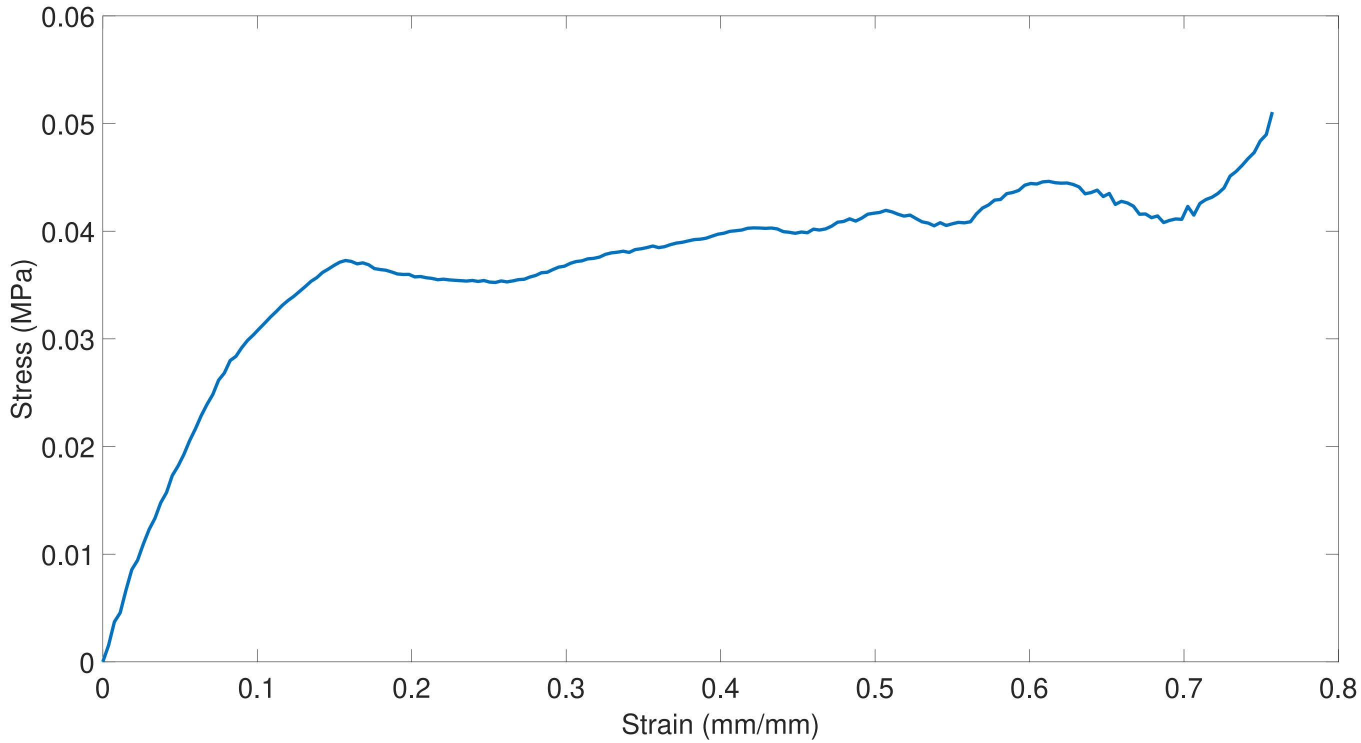

Figure 4.11 : Stress-strain graph of H7.5-L10-TH30-T0.5.

4.2.2.3 Effect of the unit cell's angle (θ)

The AuxHex structures coded as H7.5-L7.5-**TH20**-T0.5, H7.5-L7.5-**TH30**-T0.5, H7.5-L7.5-**TH40**-T0.5 are investigated here to observe the effect of the unit cell's angle (θ) on AuxHex structures' energy absorption capability. Importantly, only the parameter θ is varied, taking values of 20°, 30°, and 40° while other design parameters *h, l,* and *t* are kept as-is.

With the increased angle of unit cell (θ), energy absorptions at 10% and 25% of strain and toughness are obtained from the stress-strain graphs of FEM results are tabulated in Table 4.13.

Table 4.13 : Specific energy absorption and toughness results for increased unit cell's angle (θ).

Unit Cell Structure	$EA_{0.1}$	$EA_{0.25}$	Toughness
H7.5-L7.5-**TH20**-T0.5	166.156	454.762	1575.510
H7.5-L7.5-**TH30**-T0.5	104.388	380.272	1350.340
H7.5-L7.5-**TH40**-T0.5	67.751	313.945	1255.017

All EA and toughness results are in the unit of kJ/m^3kg.

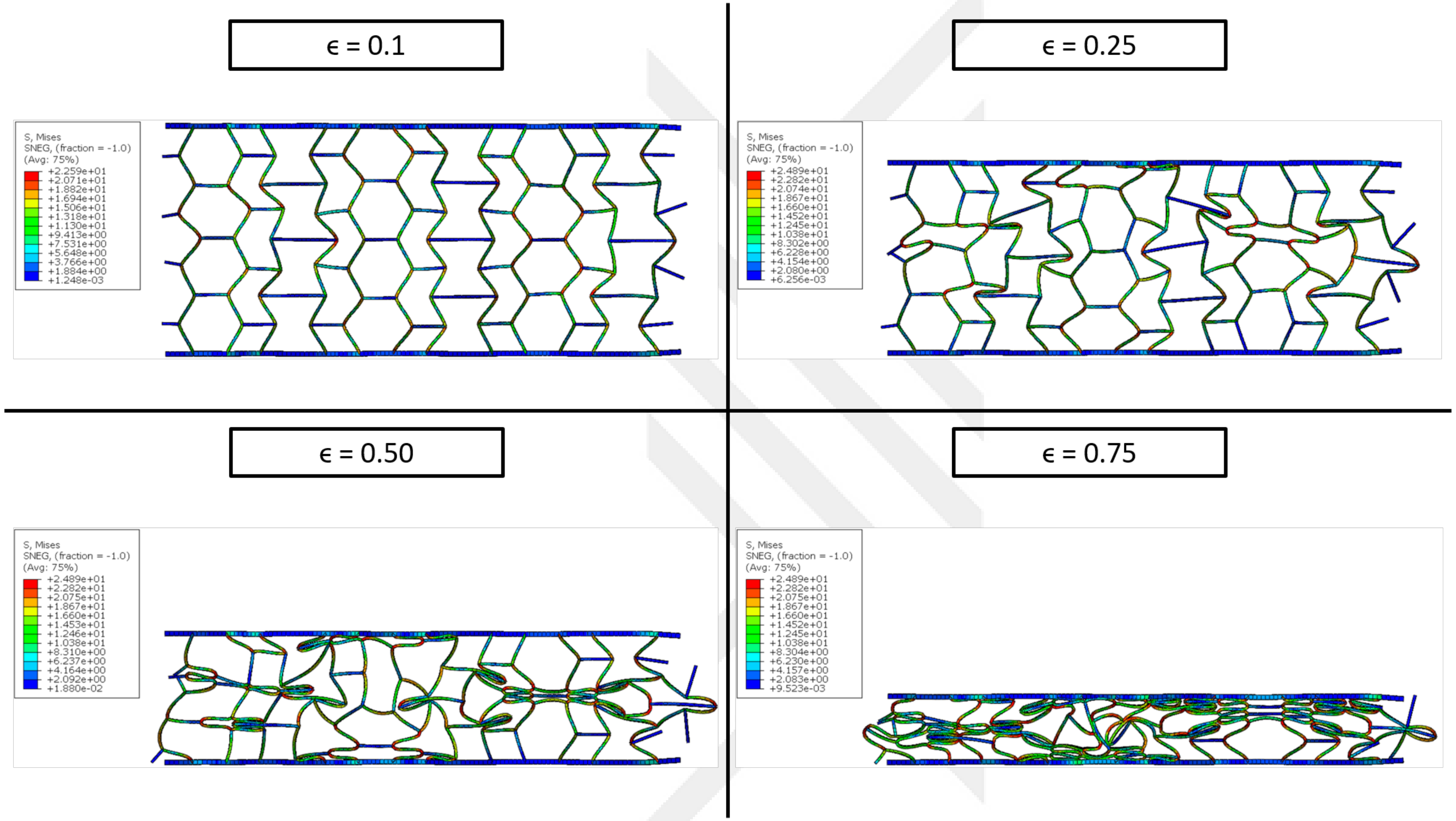

Figure 4.12 : Deformation modes of H7.5-L7.5-TH20-T0.5.

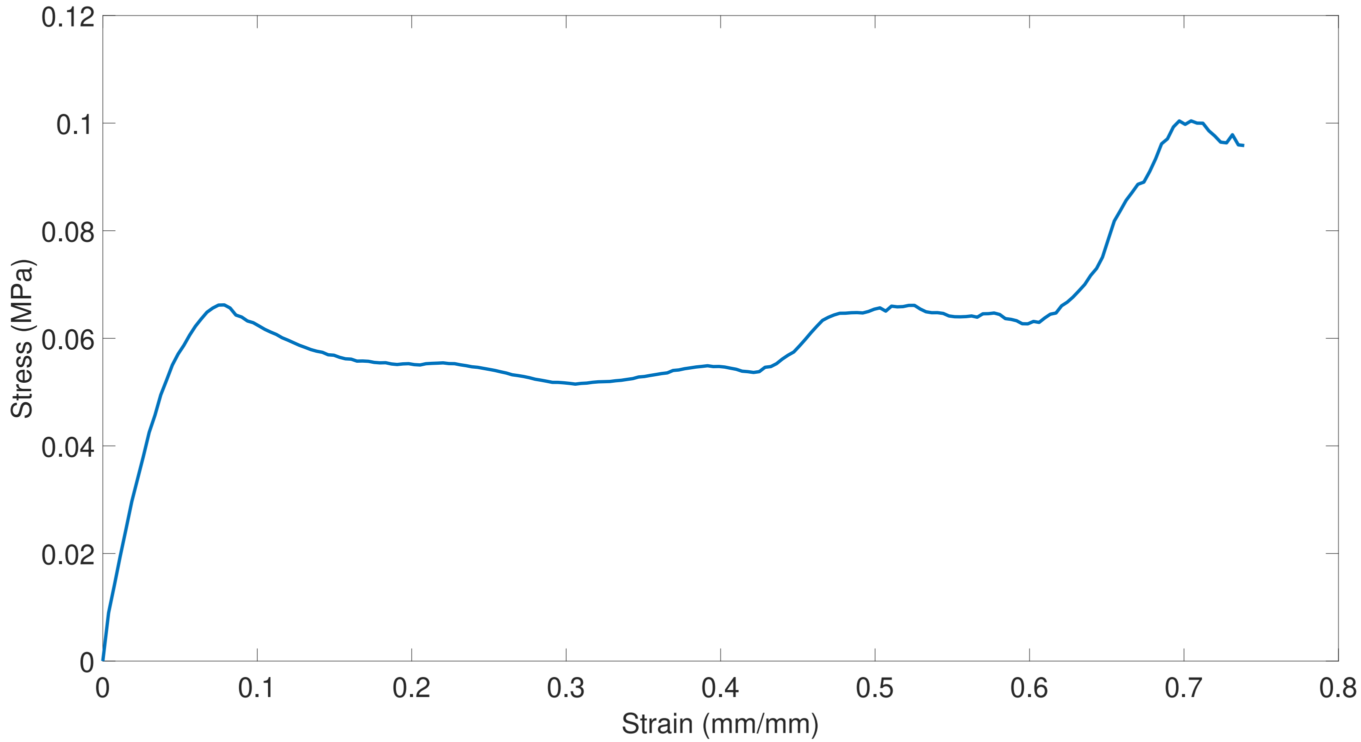

Figure 4.13 : Stress-strain graph of H7.5-L5-TH20-T0.5.

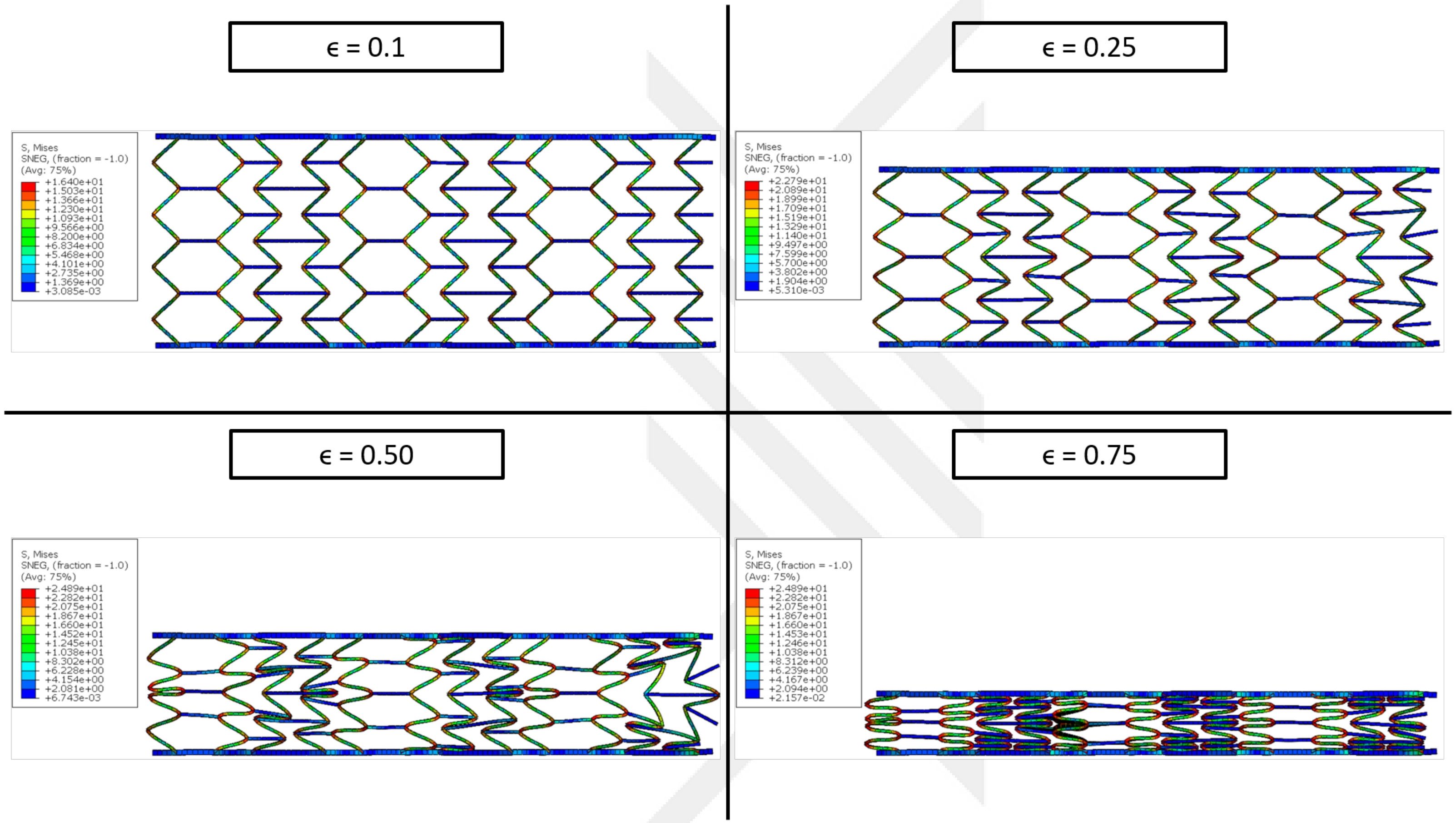

Figure 4.14 : Deformation modes of H7.5-L7.5-TH40-T0.5.

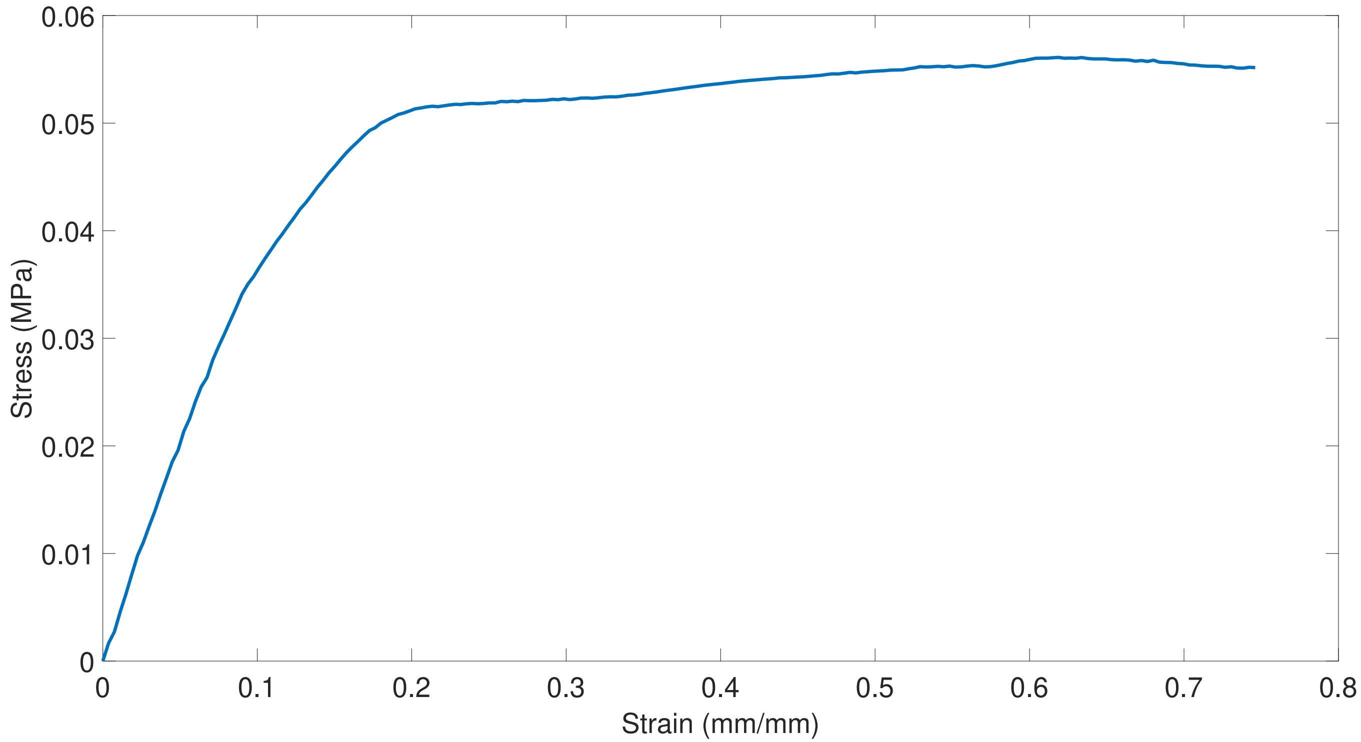

Figure 4.15 : Stress-strain graph of H7.5-L7.5-TH40-T0.5.

4.2.2.4 Effect of the thickness of unit cell's wall (*t*)

Like done in previous chapter for getting E and YS values, the AuxHex structures coded as H7.5-L7.5-TH30-**T0.4**, H7.5-L7.5-TH30-**T0.5**, H7.5-L7.5-TH30-**T0.6** are investigated here to observe the effect of increased wall thickness (*t*) of unit cell on AuxHex structures' energy absorption capability. It is crucial to note that among all design parameters, only *t* undergoes changes, assuming values of 0.4, 0.5, and 0.6 mm, while *h, l,* and θ are held constant.

With the increased wall thickness of unit cells (*t*), energy absorptions at 10% and 25% of strain and toughness are obtained from the stress-strain graphs of FEM results are tabulated in Table 4.14.

Table 4.14 : Specific energy absorption and toughness results for increased unit cell's wall thickness (*t*).

Unit Cell Structure	$EA_{0.1}$	$EA_{0.25}$	Toughness
H7.5-L7.5-TH30-**T0.4**	63.004	253.004	932.806
H7.5-L7.5-TH30-**T0.5**	104.388	380.272	1350.340
H7.5-L7.5-TH30-**T0.6**	145.000	515.476	1787.500

All EA and toughness results are in the unit of kJ/m^3kg.

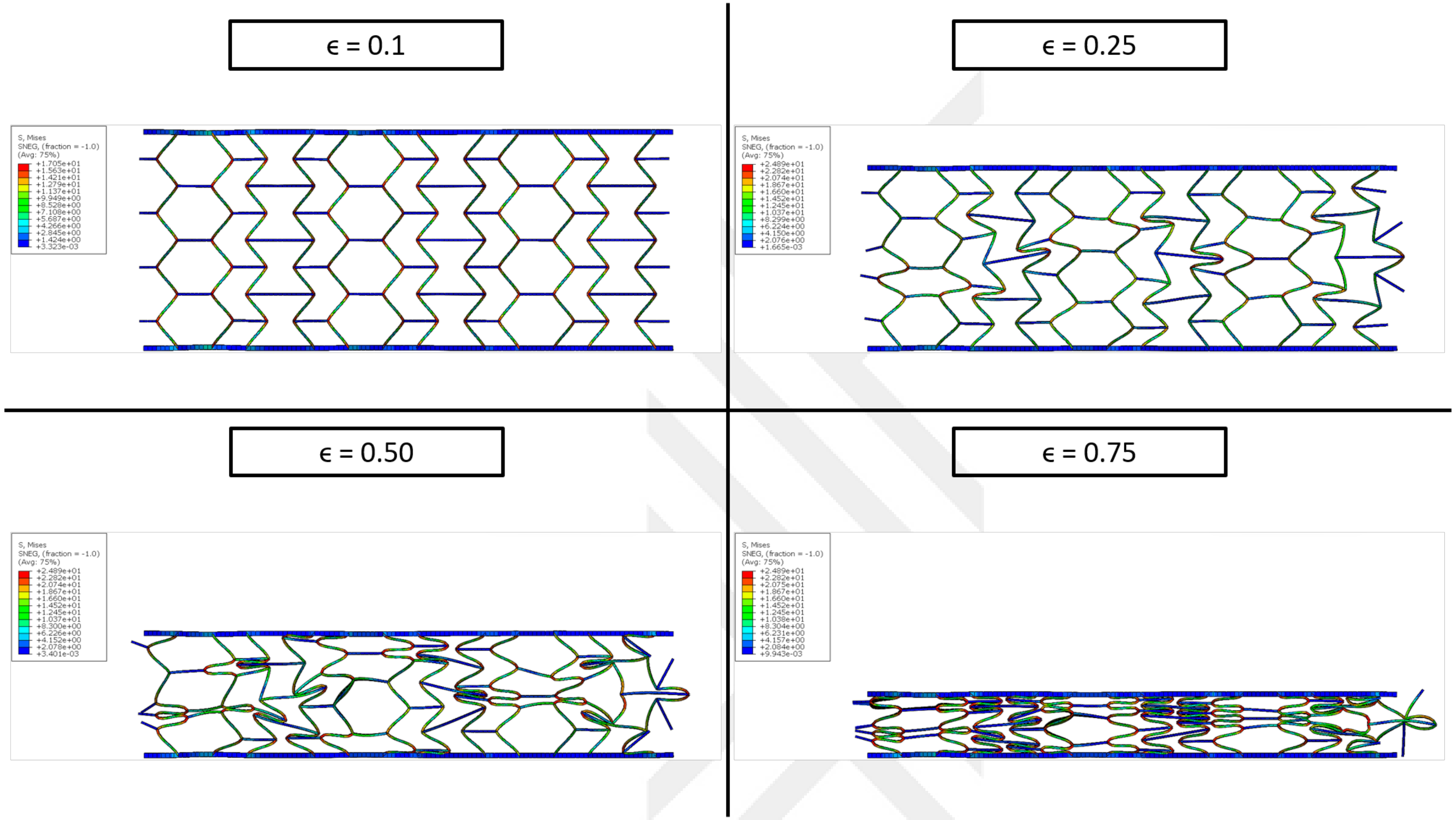

Figure 4.16 : Deformation modes of H7.5-L7.5-TH30-T0.4.

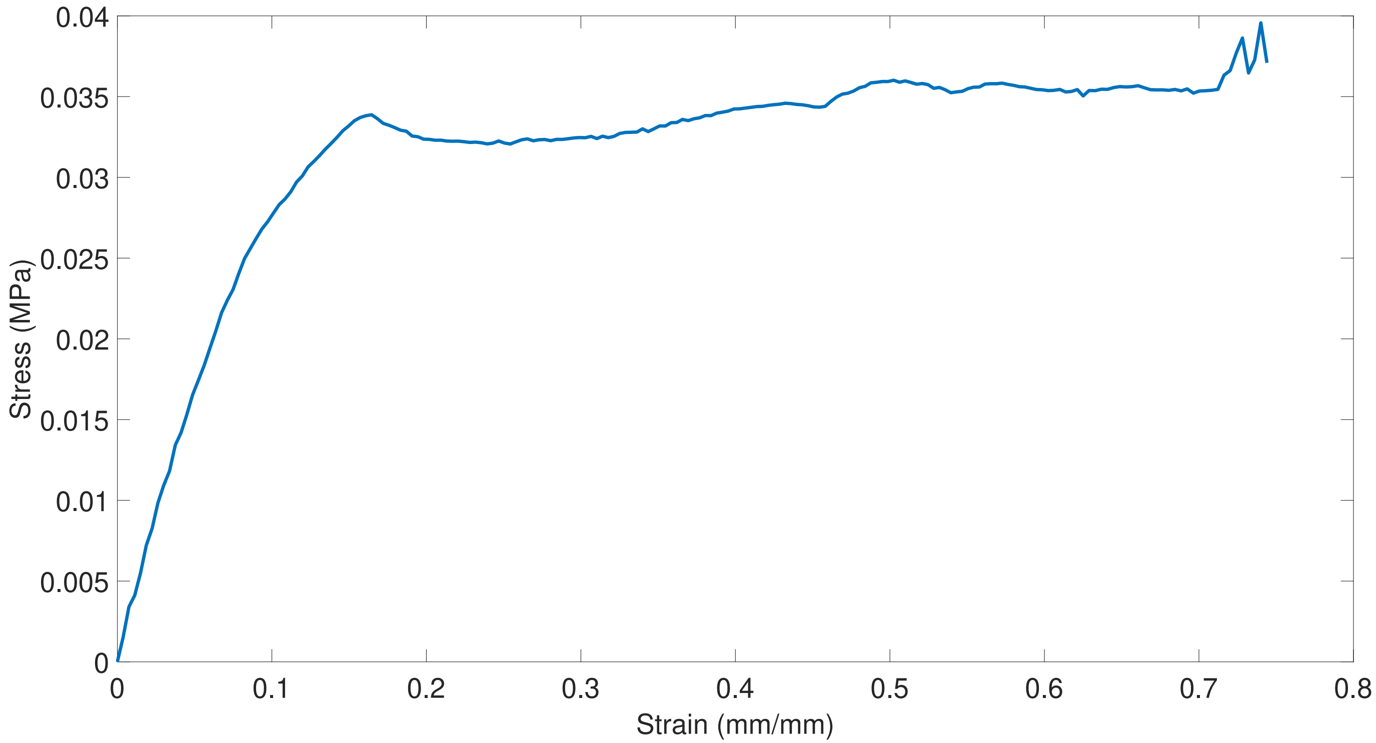

Figure 4.17 : Stress-strain graph of H7.5-L7.5-TH30-T0.4.

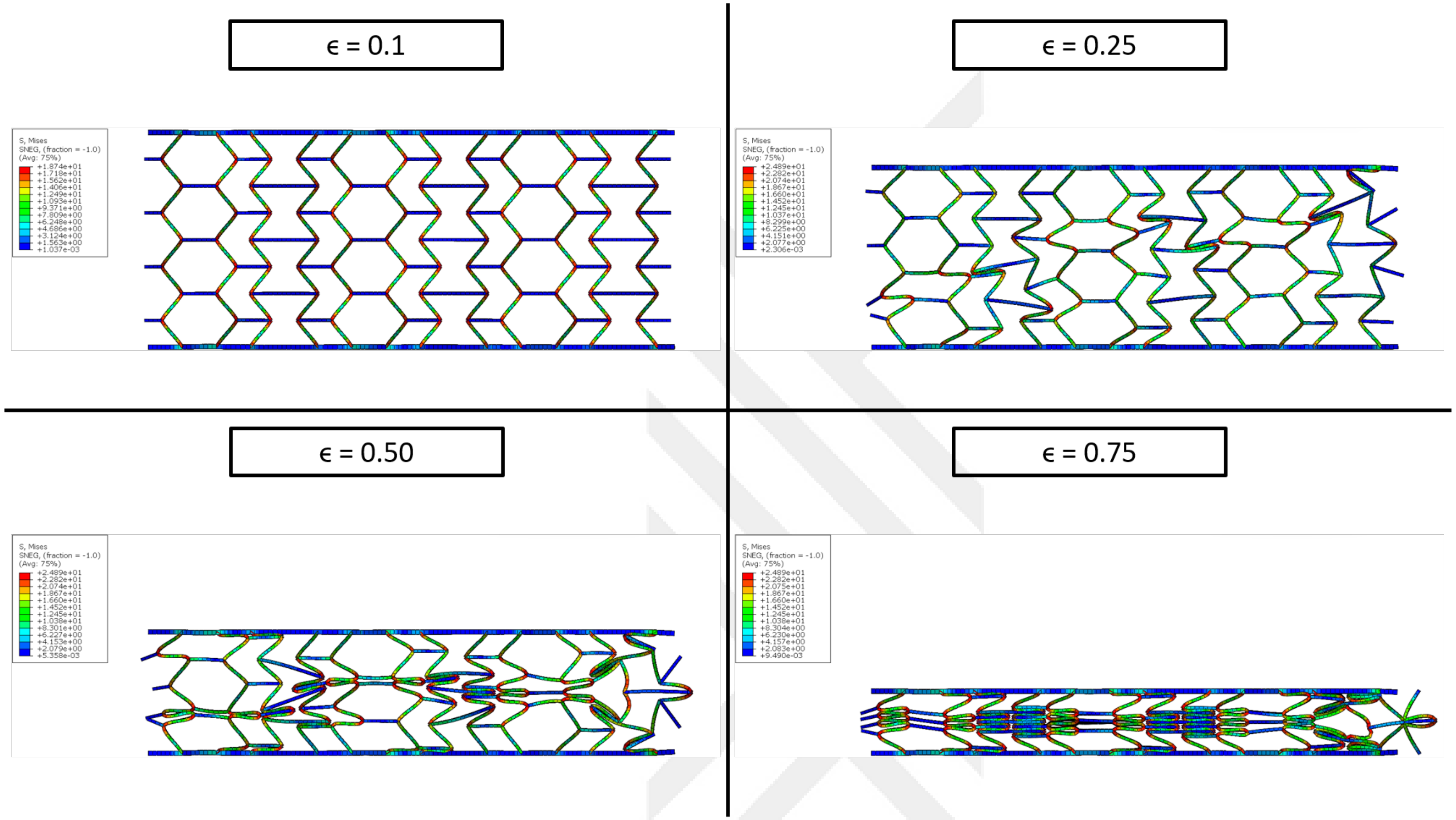

Figure 4.18 : Deformation modes of H7.5-L7.5-TH30-T0.6.

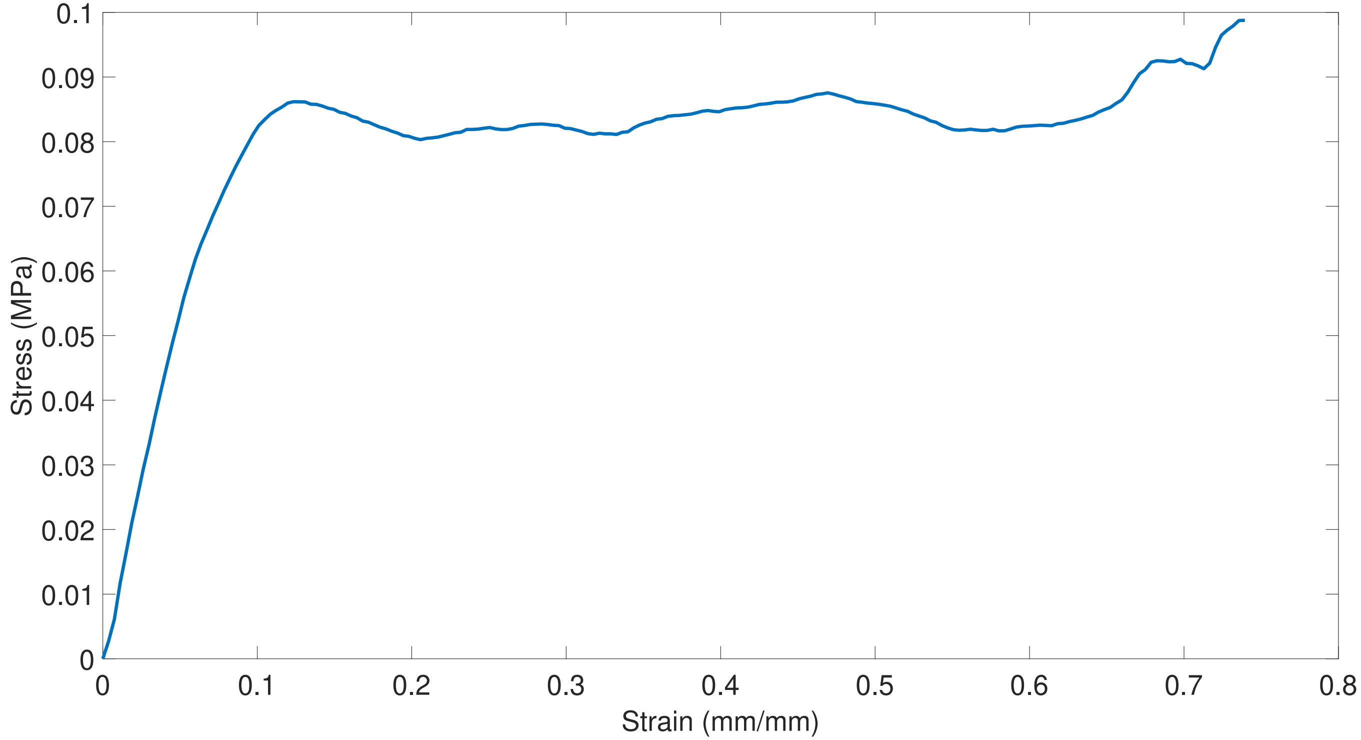

Figure 4.19 : Stress-strain graph of H7.5-L7.5-TH30-T0.6.

4.2.3 Comparison of AuxHex structures' stress-strain behaviours

Herein, the stress-strain graphs of 9 different AuxHex structures are presented. Figure 4.20 combines these stress-strain graphs in one, and shows that the collapse behaviour of structure appears to be largely related to the change in the length of non-inclined wall (*h*). Furthermore, collapse behavior can also be observed in the model H7.5-L7.5-TH20-T0.5 where unit cell's angle (θ) is 20°.

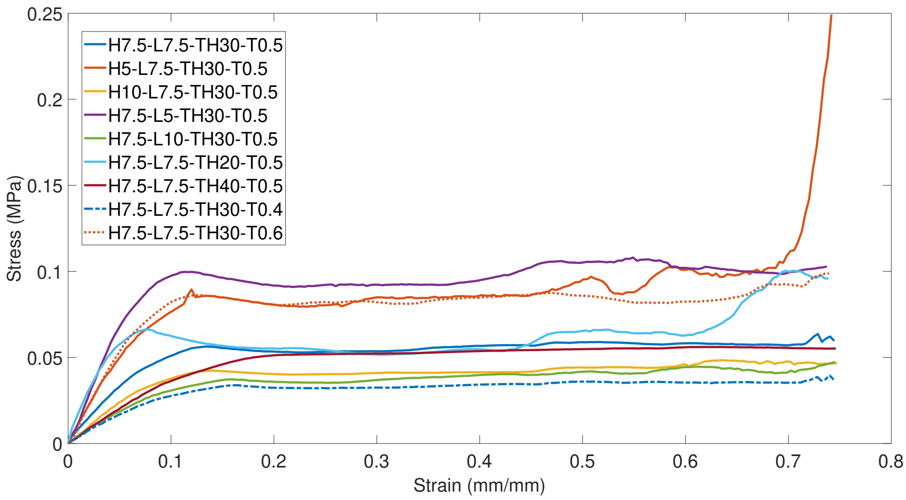

Figure 4.20 : Stress-strain graphs of all AuxHex structures.

5. CONCLUSION

In conclusion, both theoretical calculations and explicit FE analyses are performed to see the impact of AuxHex unit cells' design parameters on mechanical properties including Young's modulus, yield strength, energy absorption capacity under different strain values, and toughness.

First, analytical formulations to obtain Young's modulus and yield strength for AuxHex structure were derived and two mechanical properties (E and YS) were calculated. Meanwhile, 2D finite element models were created for nine different geometries of AuxHex sandwich structures by varying geometric parameters such as inclined and non-inclined wall cell lengths, angles, and wall thicknesses that characterize the AuxHex unit cell structure. Differences between analytical and numerical results have emerged in accordance with the examples in the literature. Secondly, energy absorption capacity and toughness values were calculated by converting force-displacement graphs into stress-strain graphs. These stress-strain graphs were integrated by using a curve fitting function in the MATLAB program to obtain the absorbed energies and toughness values at different strains values.

The analyses performed and the results obtained in this study are concluded in the following items:

1. It was observed that the Young's modulus, yield strength, energy absorption capacity, and toughness of the sandwich structure decreased with increasing inclined and non-inclined wall lengths of AuxHex unit cells.

2. All mechanical properties have increased significantly and had a positive effect on the structure with increasing AuxHex unit cell wall thicknesses.

3. The Young's modulus, yield strength, energy absorption capacity, and toughness of the AuxHex sandwich structure decreased with increasing unit cell angles used to design the AuxHex unit cells.

REFERENCES

[1] **Kassapoglou, C.** (2013). Design and analysis of composite structures: with applications to aerospace structures., John Wiley Sons.

[2] **Zheng, Z.**, **Chen, X. and Zheng, H.** (2021). Compression Performance of Composite Honeycomb Sandwich Structures with Prefabricated Defects, *International Conference on Aerospace System Science and Engineering*, Springer, pp.449–464.

[3] **Del Broccolo, S.**, **Laurenzi, S. and Scarpa, F.** (2017). AUXHEX–A Kirigami inspired zero Poisson's ratio cellular structure, *Composite Structures*, *176*, 433–441.

[4] **Günaydin, K.** (2020). Numerical and experimental investigation on the crushing behaviour of auxetic lattice cells produced with additive manufacturing techniques.

[5] **Paik, J.K.**, **Thayamballi, A.K. and Kim, G.S.** (1999). The strength characteristics of aluminum honeycomb sandwich panels, *Thin-walled structures*, *35*(3), 205–231.

[6] **Bitzer, T.**, (1997). Honeycomb core, Honeycomb Technology: Materials, Design, Manufacturing, Applications and Testing, Springer, pp.10–42.

[7] **Bruffey, N. and Shiu, W.** (2016). Predicting Flexural Strength of Composite Honeycomb Core Sandwich Panels Using Mechanical Models of Face Sheet Compressive Strength.

[8] **Obadimu, S.O. and Kourousis, K.I.** (2023). In-plane compression performance of additively manufactured honeycomb structures: a review of influencing factors and optimisation techniques, *International Journal of Structural Integrity*, *14*(3), 337–353.

[9] **Evans, K.E.** (1991). Auxetic polymers: a new range of materials, *Endeavour*, *15*(4), 170–174.

[10] **Gök, S.** (2021). *Structural design and analysis of an impact resistant auxetic metamaterial*, M. Sc. Thesis, Istanbul Technical University.

[11] **Del Broccolo, S.**, **Ouisse, M.**, **Foltete, E. and Scarpa, F.** (2018). Bandgap capability of hybrid Kirigami inspired cellular structures, *INTER-NOISE and NOISE-CON Congress and Conference Proceedings*, volume257, Institute of Noise Control Engineering, pp.681–692.

[12] **Xu, M.**, **Xu, Z.**, **Zhang, Z.**, **Lei, H.**, **Bai, Y. and Fang, D.** (2019). Mechanical properties and energy absorption capability of AuxHex structure under in-plane compression: Theoretical and experimental studies, *International Journal of Mechanical Sciences*, *159*, 43–57.

[13] **Xu, M.**, **Liu, D.**, **Wang, P.**, **Zhang, Z.**, **Jia, H.**, **Lei, H. and Fang, D.** (2020). In-plane compression behavior of hybrid honeycomb metastructures: Theoretical and experimental studies, *Aerospace Science and Technology*, *106*, 106081.

[14] **Yu, X.**, **Zhou, J.**, **Liang, H.**, **Jiang, Z. and Wu, L.** (2018). Mechanical metamaterials associated with stiffness, rigidity and compressibility: A brief review, *Progress in Materials Science*, *94*, 114–173.

[15] **Zhang, J. and Ashby, M.** (1992). The out-of-plane properties of honeycombs, *International journal of mechanical sciences*, *34*(6), 475–489.

[16] **Ashby, M.F.** (2006). The properties of foams and lattices, *Philosophical Transactions of the Royal Society A: Mathematical, Physical and Engineering Sciences*, *364*(1838), 15–30.

[17] **Sarvestani, H.Y.**, **Akbarzadeh, A.**, **Niknam, H. and Hermenean, K.** (2018). 3D printed architected polymeric sandwich panels: Energy absorption and structural performance, *Composite Structures*, *200*, 886–909.

[18] **Sun, G.**, **Huo, X.**, **Chen, D. and Li, Q.** (2017). Experimental and numerical study on honeycomb sandwich panels under bending and in-panel compression, *Materials & Design*, *133*, 154–168.

[19] **Khan, M.**, **Baig, T. and Mirza, S.** (2012). Experimental investigation of in-plane and out-of-plane crushing of aluminum honeycomb, *Materials Science and Engineering: A*, *539*, 135–142.

[20] **Wang, Z.**, **Qin, Q.**, **Chen, S.**, **Yu, X.**, **Li, H. and Wang, T.** (2017). Compressive crushing of novel aluminum hexagonal honeycombs with perforations: experimental and numerical investigations, *International Journal of Solids and Structures*, *126*, 187–195.

[21] **Combescure, C. and Elliott, R.S.** (2017). Hierarchical honeycomb material design and optimization: Beyond linearized behavior, *International Journal of Solids and Structures*, *115*, 161–169.

[22] **Fu, M.H.**, **Chen, Y. and Hu, L.L.** (2017). A novel auxetic honeycomb with enhanced in-plane stiffness and buckling strength, *Composite Structures*, *100*(160), 574–585.

[23] **Lakes, R.** (1987). Foam structures with a negative Poisson's ratio, *Science*, *235*(4792), 1038–1040.

[24] **Huang, J.**, **Zhang, Q.**, **Scarpa, F.**, **Liu, Y. and Leng, J.** (2017). In-plane elasticity of a novel auxetic honeycomb design, *Composites Part B: Engineering*, *110*, 72–82.

[25] **Evans, K.E.**, **Nkansah, M.**, **Hutchinson, I. and Rogers, S.** (1991). Molecular network design, *Nature*, *353*(6340), 124–124.

[26] **Ingrole, A.**, **Hao, A. and Liang, R.** (2017). Design and modeling of auxetic and hybrid honeycomb structures for in-plane property enhancement, *Materials & Design*, *117*, 72–83.

[27] **Ma, C.**, **Lei, H.**, **Liang, J.**, **Wu, W.**, **Wang, T. and Fang, D.** (2018). Macroscopic mechanical response of chiral-type cylindrical metastructures under axial compression loading, *Materials & Design*, *158*, 198–212.

[28] **Zhang, J.**, **Lu, G.**, **Ruan, D. and Wang, Z.** (2018). Tensile behavior of an auxetic structure: Analytical modeling and finite element analysis, *International Journal of Mechanical Sciences*, *136*, 143–154.

[29] **Günaydın, K.**, **Rea, C. and Kazancı, Z.** (2022). Energy absorption enhancement of additively manufactured hexagonal and re-entrant (auxetic) lattice structures by using multi-material reinforcements, *Additive Manufacturing*, *59*, 103076.

[30] **Yang, W.**, **Li, Z.M.**, **Shi, W.**, **Xie, B.H. and Yang, M.B.** (2004). Review on auxetic materials, *Journal of materials science*, *39*, 3269–3279.

[31] **Harkati, E.**, **Daoudi, N.**, **Bezazi, A.**, **Haddad, A. and Scarpa, F.** (2017). In-plane elasticity of a multi re-entrant auxetic honeycomb, *Composite Structures*, *180*, 130–139.

[32] **Chen, Y.**, **Scarpa, F.**, **Liu, Y. and Leng, J.** (2013). Elasticity of anti-tetrachiral anisotropic lattices, *International Journal of Solids and Structures*, *50*(6), 996–1004.

[33] **Parsons, E.M.** (2019). Lightweight cellular metal composites with zero and tunable thermal expansion enabled by ultrasonic additive manufacturing: Modeling, manufacturing, and testing, *Composite Structures*, *223*, 110656.

[34] **Lee, J.**, **Choi, J. and Choi, K.** (1996). Application of homogenization FEM analysis to regular and re-entrant honeycomb structures, *Journal of Materials Science*, *31*, 4105–4110.

[35] **Gibson, L.J.** (2003). Cellular solids, *Mrs Bulletin*, *28*(4), 270–274.

[36] **Sun, Y. and Pugno, N.M.** (2013). In plane stiffness of multifunctional hierarchical honeycombs with negative Poisson's ratio sub-structures, *Composite Structures*, *106*, 681–689.

[37] (2020). *ABAQUS 2020*, Dassault Systèmes Simulia Corp.

[38] **URL-1**. https://www.epfl.ch/schools/sti/ateliers/wp-content/uploads/2018/05/sls_PA2200_EOS.pdf, date retrieved: 05.05.2024.

[39] **URL-2**. https://www.3dprint-uk.co.uk/material-pa2200-nylon/, date retrieved: 05.05.2024.

[40] **Liu, W.**, **Wang, N.**, **Luo, T. and Lin, Z.** (2016). In-plane dynamic crushing of re-entrant auxetic cellular structure, *Materials & Design*, *100*, 84–91.

[41] **Bhardwaj, S. and Mishra, D.K.** (2024). Effect of different strut thickness on the mechanical behaviour of 3D printed auxetic structures, *Materials Today: Proceedings*.

[42] **MATLAB** (2017). *R2017b*, The MathWorks Inc.

CURRICULUM VITAE

Name SURNAME: Kadircan SAYGI

EDUCATION:

- **B.Sc.:** 2020, Istanbul Technical University, Faculty of Aeronautics and Astronautics, Department of Astronautical Engineering

PROFESSIONAL EXPERIENCE AND REWARDS:

- 2020-2022, Turkish Aerospace Industries (TAI) - Structural Analysis Engineer
- 2022 - Present, GE Aerospace - Design Engineer

PUBLICATIONS, PRESENTATIONS AND PATENTS ON THE THESIS:

- **Saygı K.**, Yildiz K. (2024). AuxHex Birim Hücreli Sandviç Yapıların Mekanik Özelliklerinin Parametrik Olarak İncelenmesi. *Ulusal Havacılık ve Uzay Konferansı*, September 18-20, 2024 Ankara, Turkey.